

**UNIVERSITY OF TURKISH AERONAUTICAL ASSOCIATION
INSTITUTE OF SCIENCE AND TECHNOLOGY**

**VOLTAGE STABILITY ANALYSIS WITH DIFFERENT TYPES OF SMALL
SIZE GENERATORS INTEGRATED IN POWER DISTRIBUTION
NETWORK**



MASTER THESIS

Weam Hussein Ali Al - TAMEEMI

**A THESIS SUBMITTED IN PARTIAL FULFILLMENT OF THE
REQUIREMENTS FOR THE DEGREE OF
MASTER OF SCIENCE IN
ELECTRICAL POWER ENGINEERING**

NOVEMBER, 2017

**UNIVERSITY OF TURKISH AERONAUTICAL ASSOCIATION
INSTITUTE OF SCIENCE AND TECHNOLOGY**

**VOLTAGE STABILITY ANALYSIS WITH DIFFERENT TYPES OF SMALL
SIZE GENERATORS INTEGRATED IN POWER DISTRIBUTION
NETWORK**



MASTER THESIS

Weam Hussein Ali Al - TAMEEMI

1406030018

**A THESIS SUBMITTED IN PARTIAL FULFILLMENT OF THE
REQUIREMENTS FOR THE DEGREE OF
MASTER OF SCIENCE IN
ELECTRICAL POWER ENGINEERING**

Supervisor: Prof. Dr. Dođan ÇALIKOĐLU

Weam AL- TAMEEMI, having the student number 1406030018 and enrolled in the Master Program at the institute of Science and Technology at the University of Turkish Aeronautical Association, after meeting all of the required conditions contained in the related regulations, has successfully accomplished, in front of the jury, the presentation of the thesis prepared with the title of: “Voltage Stability Analysis With Different Types Of Small Size Generators Integrated In Power Distribution Network”.

Supervisor : Prof. Dr. Dođan ALIKOĐLU

University of Turkish Aeronautical Association

Jury Members : Assoc. Prof. Dr. Ahmet KARAARSLAN

Yildirim Beyazit University

: Asst. Prof. Dr. İbrahim MAHARIQ

University of Turkish Aeronautical Association

: Prof. Dr. Dođan ALIKOĐLU

University of Turkish Aeronautical Association

Thesis Defense Date: 15 November 2017

**UNIVERSITY OF TURKISH AERONAUTICAL ASSOCIATION
INSTITUTE OF SCIENCE AND TECHNOLOGY**

I hereby declare that all the information in this study I presented as my Master's Thesis, called: "Voltage Stability Analysis With Different Types Of Small Size Generators Integrated In Power Distribution Network". has been presented in accordance with academic rules and ethical conduct. I also declare and certify on my honor that I have fully cited and referenced all the sources I made use of in this present study.



15.11.2017

Weam Al- TAMEEMI

AKNOWLEDGEMENT

First of all, I present my thanks to my God, who makes me able to complete this work.

I would like to present my sincere gratitude to my supervisor “Prof. Dr. Doğan ÇALIKOĞLU” for his support, helpful advice, and guidance during supervision for this work.

My special thanks to the Staff Members of Department of Electrical and Electronics Engineering who gave me continuous help.

I would like also to thank my Parents and my family for their great supports and encouragement.

November 2017

Weam Hussein Al – TAMEEMI

TABLE OF CONTENTS

AKNOWLEDGEMENT	iv
TABLE OF CONTENTS	v
LIST OF FIGURES	vii
LIST OF TABLES	ix
LIST OF ABBREVIATIONS	x
ABSTRACT	xii
ÖZET	xiii
CHAPTER ONE	1
1. INTRODUCTION	1
1.1 Presentation of the work	1
1.2 Small Size Generators.....	2
1.2.1 The Importance of the SSG units	2
1.2.2 The Types of the SSG Units.....	2
1.3 Literature Survey Class-1	3
1.4 Literature Survey Class-2	3
1.5 Thesis Aspects	5
1.6 Thesis Outline	7
CHAPTER TWO	8
2. TYPES OF THE SSG UNITS AND VOLTAGE STABILITY	8
1.2 Introduction.....	8
2.2 Small Size Generators Energy Sources.....	8
2.2.1 Photovoltaic	9
2.2.2 Wind Turbines	11
2.2.3 Fuel Cells.....	14
2.2.4 Micro – Turbines	17
2.2.5 Reciprocating Internal Combustion Engine (ICE)	18
2.2.6 Power Storage Units	18
2.3 Voltage Stability	19
2.3.1 Classification of the VS.....	19
2.3.2 Voltage Disturbances.....	20
2.4 Impacts of the SSG Units on Voltage Profile and Voltage Stability	21
CHAPTER THREE	23
3. MODELING AND ANALYSIS USING MATLAB / PSAT	23
3.1 Introduction.....	23
3.2 An Open source Power System Analysis Toolbox (PSAT).....	23
3.3.1 Slack and Load Buses Model	25
3.3.2 Transmission Line Model.....	26
3.3.3 PQ Load Model	26
3.4 PV Generator Model.....	27
3.5 PQ Generator Model.....	27
3.6 Photovoltaic Generator Model.....	27
3.7 Fuel Cell Model	28

3.8	Constant Speed SCIG Wind Turbine Model	29
3.9	Synchronous Generator Model	30
3.10	Voltage Stability Analysis Methods	31
3.10.1	Power Flow Solver	31
3.10.2	Static Analysis Method.....	32
3.10.3	Dynamic Analysis Method.....	33
3.10.4	Proximity to Voltage Instability Analysis Method.....	35
3.11	Optimum Location and Size of SSG Units	36
	CHAPTER FOUR.....	38
4.	SIMULATION AND RESULTS	38
4.1	Introduction.....	38
4.2	Distribution Network Model Simulation	39
4.3	Network Power Flow Analysis (without SSG unit).....	40
4.4	Optimum Location and Capacity of SSG Units.....	43
4.5	Voltage Stability Static Analysis Results	45
4.5.1	Photovoltaic SSG Unit (PVG).....	46
4.5.1.1	Voltage Control Operation Mode	46
4.5.1.2	Power factor control operation mode	47
4.5.2	Reactive Power Control Operation Mode	47
4.5.3	Solid Oxide Fuel Cell SSG.....	48
4.5.4	Constant Speed Wind Turbine with Induction generator Model.....	49
4.5.5	Synchronous Generator Model.....	50
4.5.6	Discussion of the Static Analysis Results	51
4.6	Voltage Stability Dynamic Analysis Results.....	51
4.6.1	Network Dynamic Analysis without SSG unit.....	51
4.6.2	Network Dynamic Analysis with a FC-SSG Unit.....	52
4.6.3	Network Dynamic Analysis With a Synch. Gen unit.....	53
4.6.4	Network Dynamic Analysis With a CSWTIG Unit	54
4.6.5	Discussion of the Dynamic Analysis Results.....	56
4.7	Small Signal Stability Analysis SSSA Results	57
4.7.1	Network With a FC-SSG Unit.....	57
4.7.2	Network With a Synch. Gen Unit.....	58
4.7.3	Network With a WTIG Unit.....	59
4.7.4	Discussion of the SSSA Results	61
	CHAPTER FIVE.....	62
5.	CONCLUSIONS AND SUGGESTIONS FOR FUTURE WORK	62
5.1	Conclusions.....	62
5.2	Suggestions For Future Work	64
	REFERENCES.....	65
	APPENDICES	71
	Appendix-A: Lines and Loads Data of the 33-Bus Radial Distribution Network	72
	Appendix-B: Power Flow Report of the network (without SSG)	73
	Appendix C: FC-SSG standard parameters.....	77
	Appendix-D: Eigenvalue Report of the a FC-SSG.....	82
	CURRICULUM VITAE.....	85

LIST OF FIGURES

Figure 2.1	: SSG energy sources.....	9
Figure 2.2	: P-V characteristics and I-V characteristics of a silicon solar cell. Also shown is the (MPP) at V_{mp} and I_{mp}	10
Figure 2.3	: Grid connected photovoltaic generator.	11
Figure 2.4	: Types of wind turbines.	12
Figure 2.5	: Fixed speed SCIG wind turbine equivalent circuit.....	14
Figure 2.6	: Operation principle of the fuel cell.....	15
Figure 2.7	: FC equivalent circuit.	16
Figure 2.8	: Classification of power system stability.....	19
Figure 3.1	: PSAT main graphical user interface.....	24
Figure 3.2	: 33-bus radial distribution network model.....	25
Figure 3.3	: Transmission line π circuit.	26
Figure 3.4	: Equivalent circuit of photovoltaic grid-connected system.	28
Figure 3.5	: Fuel cell generator with (VSI) Inverter.	29
Figure 3.6	: Squirrel cage induction generator equivalent circuit.....	30
Figure 3.7	: λ -V curve.	33
Figure 3.8	: Time domain integration block diagram.	34
Figure 3.9	: A System poles locations in the S domain.	36
Figure 4.1	: Main steps of the proposed work.....	39
Figure 4.2	: Single line Model of 33-bus radial network (base case).	40
Figure 4.3	: GUI of CPF network visualization.	41
Figure 4.4	: Voltage stability margin (without SSG).	42
Figure 4.5	: P-V Curves (without SSG).	42
Figure 4.6	: Network total power losses with SSG at different busses.....	44
Figure 4.7	: Optimum SSG unit capacity.....	45
Figure 4.8	: Integration Impact of a PV Generator using GUI.	46
Figure 4.9	: λ -V Curves when a PV generator was integrated into DN.....	47
Figure 4.10a	: DN integrated with FC-SSG model.....	48
Figure 4.10b	: λ -V curves (Network with a FC-SSG).	49
Figure 4.11a	: DN integrated with SCIG unit.....	49
Figure 4.11b	: λ -V curves for the network buses with CSWTIG unit.	50
Figure 4.12	: λ -V curves (Network with a Synch – SSG).....	50
Figure 4.13	: Earth fault model.	52
Figure 4.14	: Time domain simulation of the network without SSG.....	52
Figure 4.15	: Time domain simulation of the network with a FC-SSG.	53
Figure 4.16a	: Time domain simulation of the network with a Synch.SSG.	53
Figure 4.16b	: Time domain simulation of the network with a Synch.SSG & AVR.	54
Figure 4.17	: Voltage flicker of a CSWTIG at bus10.	54
Figure 4.18	: Time domain simulation of the network with a WTIG.....	55
Figure 4.19	: WTIG with fault and C.B models.	56

Figure 4.20 : Time domain simulation (Disconnecting WTIG)..... 56
Figure 4.21a : Eigenvalues of the FC-SSG in the S-domain axis..... 57
Figure 4.21b : Eigenvalues of the Sych.SSG in the S-domain. 58
Figure 4.21c : Eigenvalues of the WTIG in the S-domain. 59
Figure 4.22 : Hybrid model (WTIG unit & Sych.SSG)..... 60
Figure 4.23 : Eigenvalue of the hybrid model in the S-domain..... 61



LIST OF TABLES

Table 3.1	: Model Identification of the Slack and Load buses.	25
Table 4.1	: Summary report of power flow of the network (base case).	41
Table 4.2	: Summary report of CPF of the network (base case).....	41
Table 4.3	: Results of optimum SSG location.	43
Table 4.4	: The impact of optimum capacity of SSG unit on utility power and DN losses.	45
Table 4.5	: Static analysis results of the DN with static SSG models.	48
Table 4.6	: Loading parameters of the DN with different SSG unit types.	51
Table 4.7	: dynamic analysis results report for different SSG types.	57
Table 4.8	: Eigenvalues of the FC-SSG.....	58
Table 4.10	: Eigenvalues of the WTIG.....	60

LIST OF ABBREVIATIONS

AC	: Alternative Current
AFC	: Alkaline Fuel Cell
AVR	: Automatic Voltage Regulator
CB	: Circuit Breaker
CHP	: Combined Heat and Power
CPF	: Continuation Power Flow
CSWTIG	: Constant Speed Wind Turbine Induction Generator
DC	: Direct Current
DFIG	: Doubly Fed Induction Generator
SSG	: Small Size Generator
DN	: Distribution Network
DVSA	: Dynamic Voltage Stability Analysis
FACTS	: Flexible Alternating Current Transmission System
FC	: Fuel Cell
GUI	: Graphic user Interface
ICE	: Internal Compassion Engine
LSF	: Loss Sensitivity Factor
MCFC	: Molten Carbonate Fuel Cell
MINLIP	: Mixed Integer Non-Liner Programming
MPPT	: Maximum Power Point Tracking
MT	: Micro Turbine
NR	: Newton Raphson
PAFC	: Phosphoric Acid Fuel Cell
PEMFC	: Proton Exchange Membrane Fuel Cell
PMSG	: Permanent Magnet Synchronous Generator
PSAT	: Power System Analysis Toolbox
PWM	: Pulse Width Modulation
PVG	: Photovoltaic Generation
P-V	: Power-Voltage
RDN	: Radial Distribution Network
RMS	: Root Mean Squire
SCIG	: Squirrel Cage Induction Generator
SOFC	: Solid Oxide Fuel Cell
SPVG	: Solar Photovoltaic Generator
SSSA	: Small Signal Stability Analysis
SVSA	: Static Voltage Stability Analysis
Synch.SSG	: Synchronous Small Size Generator
TDS	: Time Domain Simulation
TNI	: Trapezoidal Numerical Integration
VS	: Voltage Stability
VSM	: Voltage Stability Margin

V-Q : Voltage-Reactive power
VSI : Voltage Source Inverter
WRIG : Wound Rotor Induction Generator
WRSG : Wound Rotor Synchronous Generator
WTIG : Wind Turbine Induction Generation
WTSCIG : Wind Turbine Squirrel Cage Induction Generation



ABSTRACT

VOLTAGE STABILITY ANALYSIS WITH DIFFERENT TYPES OF SMALL SIZE GENERATORS INTEGRATED IN POWER DISTRIBUTION NETWORK

Tameemi, Weam

Master, Department of Electrical and Electronics Engineering

Supervisor: Prof. Dr. Doğan ÇALIKOĞLU

November 2017, 85 page

The integration effect of different types of Small Size Generators (SSG) units on the voltage stability of a 33-bus radial distribution network has been investigated. This is because some of them have features which enhance voltage stability margins of the distribution network buses. Voltage stability analysis methods of the 33-bus radial distribution network integrating various types of SSG units into the network have been done.

The proposed work is implemented using MATLAB/Simulink. The PSAT (Power System Analysis Toolbox) has been used to determine the best type of the SSG unit that improves voltage stability and loadability of the radial distribution network. Different types of SSG units are presented; the first type is Static (Photovoltaic and Fuel Cells), the second type is Dynamic (Constant Speed Wind Turbine with Squirrel Cage Induction Generator and Synchronous Generator).

The static SSG unit types have improved the voltage stability and loadability of the radial distribution network. However, the dynamic ones have a negative impact on the voltage stability because of their dynamic nature.

Keywords: Small Size Generators, Voltage Stability, Distribution Network, Matlab, Simulink, PSAT.

ÖZET

GÜÇ DAĞITIMI ŞEBEKESİNE ENTEGRE EDİLMİŞ FARKLI TÜRLERDEKİ KÜÇÜK BOYUTLU JENERATÖRLERİLE GERİLİM DENGESİ ANALİZİ

Tameemi, Weam

Yüksek Lisans, Elektrik ve Elektronik Mühendisliği Bölümü

Tez Danışmanı: Prof. Dr. Doğan ÇALIKOĞLU

Kasım, 2017, 85 sayfa

Farklı türlerdeki Küçük Boyutlu Jeneratör (SSG) ünitelerinin 33 baralı bir radyal dağıtım sisteminin gerilim dengesi üzerinde entegrasyon etkisi araştırılmıştır. Bunun nedeni, bazılarının dağıtım şebeke baralarının gerilim dengesi sınırlarını ve toleransını arttıran özelliklere sahip olmasıdır. Çeşitli türlerdeki Küçük Boyutlu Jeneratör (SSG) ünitelerinin şebekeye entegre edilmesi ile 33 baralı radyal dağıtım şebekesinin gerilim dengesi analiz yöntemleri kullanılmıştır.

Önerilen çalışma MATLAB/Simulink kullanılarak uygulanmıştır. Radyal dağıtım şebekesinin gerilim dengesi ve yüklenebilirliğini geliştiren en iyi SSG ünitesinin belirlenmesi için PSAT (Güç Sistemi Analizi Araç Kutusu) kullanılmıştır. Birinci tip Statik (Güneş Pili ve Yakıt Pilleri), ikinci tip Dinamik (Sincap Kafesi İndüksiyon Jeneratör ve Eş Zamanlı Jeneratörlü Sabit Hızlı Rüzgar Türbini) olmak üzere farklı tiplerde SSG üniteleri sunulmuştur.

Statik SSG ünite tipleri, radyal dağıtım şebekesinin gerilim dengesi ve yüklenebilirliğini geliştirmiştir. Bununla birlikte, dinamik üniteler dinamik doğalarından dolayı gerilim dengesi üzerinde negatif bir etkiye sahiptir.

Anahtar Kelimeler: Küçük Boyutlu Jeneratörler, Gerilim Dengesi, Dağıtım Şebekesi, Matlab, Simulink, PSAT.

CHAPTER ONE

INTRODUCTION

1.1 Presentation of the work

A Small Size Generator (SSG) can be a PV, a Fuel Cell, a Synchronous generator, a wind turbine induction generator or a similar electrical energy generation device whose capacity is less than 10 MVA in general. Such SSG units are used in distribution networks by the customers to inject active power into the network and to improve the voltage stability. Each such SSG is called a local SSG with respect to the customer who owns it.

In this work, a comparative study of analytical results is made to find out the best type of SSG unit regarding the improvement in voltage stability of a 33-bus radial distribution network which was introduced by Singh et al 2007 [56]. Static and dynamic SSG units are used individually with optimum size and location. Three types of voltage analysis are performed (static, dynamic and small signal stability analysis) by using 'MATLAB/Simulink' Power System Analysis Toolbox (PSAT) programming.

The motivation of this undertaking is that every distribution network tends to lose its voltage whenever the load demand increases during the normal operation or during a disturbance. So the benefit of integrating the SSG units into distribution networks is that they help solving the problem of the limited capacity of the tap changer transformers which is utilized to compensate the voltage drop in the distribution networks.

What achieved in this work is analytical results which showed that the static SSG unit types such as a PV and a Fuel cell generators have improved the voltage stability and loadability of the distribution network. On the other hand, the dynamic ones such as synchronous and induction generators have a negative impact on the

voltage stability due to their dynamic nature. The benefit of this study is determining the SSG unit type that improves the voltage stability of the distribution network regarding the integration of the SSG units into the distribution networks.

1.2 Small Size Generators

Static and Dynamic SSG units are integrated individually into the radial distribution network in order to obtain the comparisons between the analytical results which determine the SSG unit type that enhances the VS of the distribution network.

1.2.1 The Importance of the SSG units

SSG units provide many advantages such as enhanced reliability, power quality, efficiency, reduction of system limitations along with the environmental advantages. They have much ability to improve distribution system performance. Some of the SSG unit types strongly participate to improve the VS of the distribution network. The aim of the VS analysis is to determine the SSG unit type that improves the VS of the radial distribution network.

1.2.2 The Types of the SSG Units

The SSG unit models which are used in this work as follows;

1. The Static Units

- a) PV generator model: generates constant active power and fixed voltage
- b) PQ generator model: generates active and reactive powers
- c) Q generator model : generates only reactive power
- d) Fuel Cell generator model: generates active power

2. The Dynamic Units

- a) Constant Speed Wind Turbine with a squirrel cage Induction Generator model: generates active power but consumes reactive power from the network
- b) Synchronous generator model: generates active and reactive powers

1.3 Literature Survey Class-1

The following are the main references related to the VS analysis of the distribution networks;

Ref. [1] defined the stability of power system as “a property of a power system that enables it to remain in a state of equilibrium under normal operating conditions and to regain an acceptable state of equilibrium after being subjected to a disturbance”.

In Ref. [2] the authors explained the impacts of dispersed generation on distribution networks such as voltage profile, system losses, power flow, power stability, quality, reliability, and protection. They increase the electric system complexity.

Ref. [3] classified the stability of power system into VS, frequency stability, and rotor angle stability. Furthermore, the literature classified the VS as small or large according to the disturbance sort. Small VS is the capability of the network to control the voltage when small disturbances happen, such as changing of the loads. Large VS means that the network able to control the voltage after being submitted to perturbations such as faults, sudden outages of the load, and big-step changes in the load.

Ref. [4] proposed a method of placement and sizing SSG units so as to improve the VS margin of a distribution system by using mixed integer nonlinear programming (MINLP).

Ref. [5] analyzed the impacts of the SSG units on VS by introducing a guide to locate and size the SSG units to develop the VS margin in a distribution network and investigated the influence of high penetration level of SSG units on the proximity of voltage instability.

1.4 Literature Survey Class-2

The following are the main references related to the SSG units which are integrated into distribution networks;

Ref. [6] defines SSG units as a small supply of electric power generation (its ranging from less than a kW to several of MW) that is not related to a central power system and its location is close to the load.

Ref. [7] mentioned the Internal Compassion Engine (ICE) as the most commonly used SSG technology and has the least costs among other types. (ICE) utilizes either a synchronous generator for capacity higher than (300KW) or an induction generator for capacity lower than (300KW) and they can be connected directly to the grid without any converter devices.

Ref. [8] defined SSG as the generation of electrical power by utilities which are smaller than main power plants so as connected at any point in a power system.

In Ref. [9] the authors compared the efficiency of photovoltaic generation (PVG) with that of wind turbines. The efficiency of (PVG) is still low, less than 20% and their lifetime can reach over 25 years and its efficiency decreases with aging to

(75-80)% of the rated value. The same literature discussed a fuel cell as one of the available technologies and regarded alike to a battery. But it differs from a battery in that it does not require to be charged because its resources are continuously supplied to the cell, it is unlike a battery which its materials are consumed during the electrochemical process. Full Cells efficiency is high, about (40-60)% when used for power generation. Furthermore, when the exothermic heat is combined with electrical power (CHP), the total efficiency can be more than 80%. The benefits of fuel cells are their small footprint, noiseless operation, and harmful emissions during operation are not exist.

Ackerman [10] classifies wind turbines into four types, one of them is a constant speed wind turbine with a squirrel cage induction generator (SCIG) integrated directly to the grid using a transformer. In this type, if the grid is a weak, variations in wind speed transformed to electrical power fluctuations which cause voltage flicker. Other three types are variable speed wind turbines. The second type uses wound rotor induction generator (WRIG). In this sort, the generator speed supposed to be increased up to 10% above the synchronous speed of the network.

Ref. [11] presented another type of SSG 'Micro-turbines' are a combination of small (generator and turbine), they differ from the normal combustion turbines in that their speed is very high, about (50,000-120,000) rpm, in the range. Their advantages are that they are small in size, so they are suitable in a small area, low gas emission, low noise, low installation and maintenance costs, and high efficiency. They require power electronics converter (ac-dc-as converter) because they generate a very high -

frequency power, in the range of (1500-4000 Hz) in order to integrate them into the grid or to connect them synchronously with other types of SSG power sources.

Li-Shiang et.al. [12] discussed the interfacing of Photovoltaic SSG units to the power network by utilizing electronic converters with Maximum Power Point Tracking (MPPT).

The authors in Ref. [13] divided the interface of SSG units into two types; Direct grid-connected units that consist of synchronous generators and induction generators. The second type is Indirect grid-connected units which used when the output power of the generator is DC such as photovoltaic, fuel cells, high - frequency AC source such as micro-turbines, and variable frequency such as wind turbines which have power electronics converters.

Ref. [14] grouped SSG units into four major types based on terminal characteristics in terms of real and reactive power delivering capability. The first type is capable of generating only active power such as photovoltaic, micro turbines, fuel cells, which are connected to the main grid with the support of converters/inverters. However, according to the current situation and grid modes, the photovoltaic generator can provide reactive power as well. The second type is able to generate both active and reactive power. SSG units such as synchronous machines (cogeneration, gas turbine, etc.) classified under this type. The third type is capable of delivering only reactive power. Synchronous compensators such as gas turbines are the example of this type and operate at zero power factors. The fourth type generate active power but consume reactive power. Induction generators, which are used in wind turbines, come under this class. However, doubly fed induction generator (DFIG) systems may absorb or generate reactive just like a synchronous generator.

1.5 Thesis Aspects

The work is consist of the following steps:-

1. Modeling a 33-bus radial distribution network and 32 constant load feeders using (PSAT) programming.
2. Determining the optimum location and capacity of the SSG units using Loss Sensitivity Factor (LSF) method, in order to execute the analysis efficiently.

3. Integrating four types of SSG units individually. Two types are Static Generation (Photovoltaic and Fuel Cells), and other two types are dynamic Generation (Synchronous Generator and Constant Speed with Squirrel Cage Induction Generator Wind Turbine).
4. Performing the Static Voltage Stability Analysis (SVSA) on the model using power Flow calculations (Newton-Raphson) method and Continuation Power Flow (CPF) technique.
5. Implementing the Dynamic Voltage Stability Analysis (DVSA) on the model using Time Domain Simulation (TDS) solved by Trapezoidal Numerical Integration (TNI) method when the model was subjected to a fault disturbance at the weakest bus voltage.
6. Investigating the Proximity to Voltage Instability of the network using Small Signal Stability Analysis (SSSA) which is achieved in the frequency domain using Eigenvalue analysis.
7. Comparing the analysis results for each proposed SSG unit type to select the best one that enhances the voltage stability of radial distribution network during normal operation condition and perturbation condition such as an earth fault.

Referring to the R. S.A.Abri, E.F.El-Saadany, and Y.M.Atwa, 2011 [4] which proposed a method of placement and sizing SSG units so as to improve the VS margin of a distribution system by using mixed integer nonlinear programming (MINLP). In this work, the contribution is determining the optimum location and size of DG units using Loss Sensitivity Factor (LSF) method in order to improve the VS margin.

R. Al-Abri, 2012 [5] analyzed the impacts of the SSG units on VS and investigated the influence of high penetration level of them on the proximity of VS. On the other hand, the contribution of this proposed work is to select the best SSG unit type that enhances the VS of the RDN during normal operation condition and disturbance condition such as an earth fault using Power System Analysis Toolbox (PSAT) in MATLAB.

1.6 Thesis Outline

The thesis is organized in five chapters as follows:

1. Chapter one introduces a general introduction of different types of SSG units, main component of the work, literature survey, thesis objectives, and thesis outline.
2. Chapter two presents the theoretical background and basic principles of different types of SSG units and their impacts on system stability. Voltage contingencies types in distribution network were presented. Also, this chapter explains different methods of VS analysis.
3. Chapter three covers the mathematical models of different types of SSG units and modeling 33-bus RDN. Also, it covers the numerical analysis of the voltage stability.
4. Chapter four introduces the simulation results and discussion of VS analysis results with integration of different types of SSG units into RDN.
5. Chapter five presents a summary of the work conclusions and presents some suggestions for future work.

CHAPTER TWO

TYPES OF THE SSG UNITS AND VOLTAGE STABILITY

1.2 Introduction

SSG units are electric power generation source integrated into the DN or near the customer side to support the economic operation of the distribution grid. They are relatively small generation units ‘a few kilowatts up to 50 MW’, smaller than central generating plants so as to allow interconnection at any point in power system [15].

It is obvious that SSG unit is not a completely recent invention. Utilities had their own assigned geographical regions, generating and distributing electricity locally. Central grids then came along to make large interconnected systems that made electric power systems more economical, reliable, and robust. Recent interests are growing in the power industry today. For instance, although hydro power plants are considered to be environmentally friendly, it is very hard to find new locations for hydro power station installations in most regions. This issue, prevalence of power systems and dramatically growing demand for electricity have made SSG the desired choice that has been pondered by many utilities in the recent electricity market such as customers, power distributors, power producers, regulators and researchers [16].

Recently, the SSG in distribution networks has raised to high levels, and their impact on the VS has become crucial.

2.2 Small Size Generators Energy Sources

The main sources utilized in SSG technology are shown in Figure (2.1) as follows:

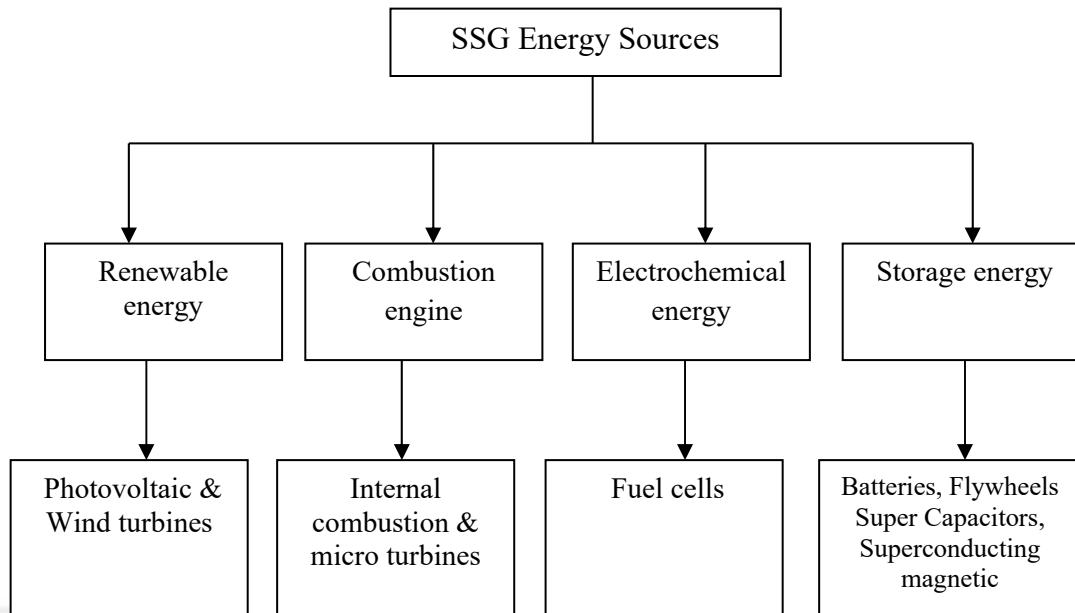


Figure 2.1: SSG energy sources.

2.2.1 Photovoltaic

Photovoltaic (PV) is the direct transfer of solar rays into electricity. Photovoltaic has a significant position among renewable energies. PV technology is modular (existing systems are expandable), its life time up to 25 years, silent and emission-free during operation [17].

A solar cell is a huge-size semiconductor diode. Sun light falling into the semiconductor produces pairs of electron-hole, leading to increasing the accumulation of the minority charge carriers by several orders of magnitude. These charge carriers disperse

to the gap charge region and are separated by the electric field there. a potential V is detected amid the contacts of the n-side and p-side. A current I passes through an applied load resistor R , and electrical power is produced.

The achievable power P_{MAX} is known the maximum achievable result of V and I at a working point:

$$P_{MAX} = P_{mp} = I_{mp} \cdot V_{mp} \quad (1)$$

The “Maximum Power Point” (MPP) is specified by I_{mp} and V_{mp} . The relation of P_{MAX} to P_{opt} is known “the fill factor” (FF). It determines the shape “rectangularness” of the draw of the feature. Figure (2.2) shows the active power P as a function of the potential V and (I-V) characteristic curve.

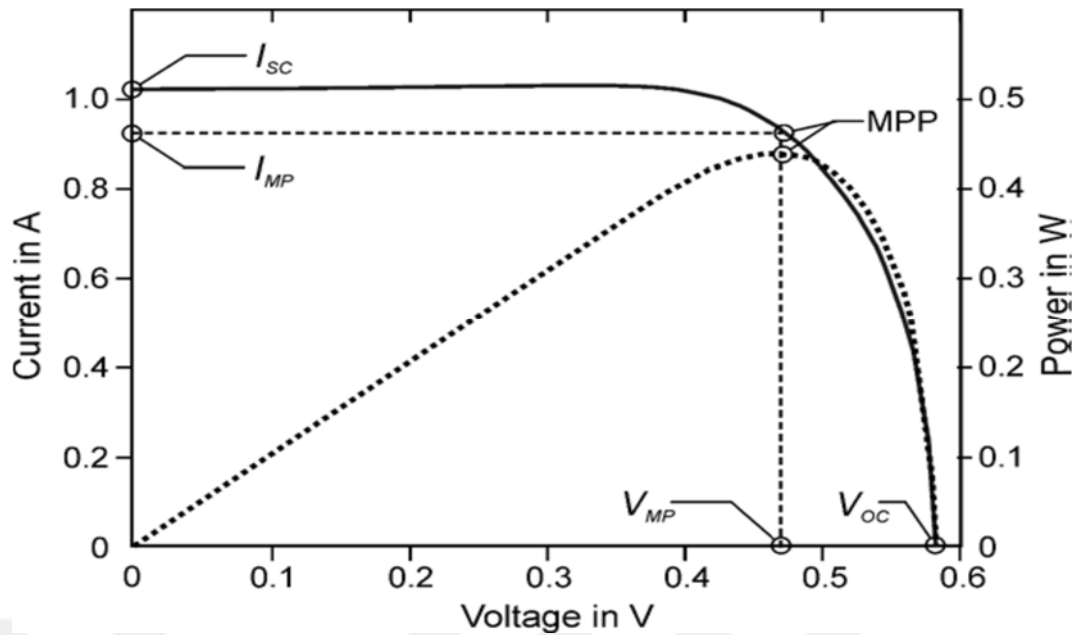


Figure 2.2: P-V characteristics and I-V characteristics of a silicon solar cell. Also shown is the (MPP) at V_{mp} and I_{mp}

In comparing choice power generation methods, the delivered energy cost per kilowatt hour is the most essential measure. In PVG power, this cost depends on two factors: the efficiency of the PVG energy conversion, and main cost per watt capacity. Together, the economic competitiveness of the PVG electricity indicated by these two factors [18].

The practical structure of a grid-connected photovoltaic generator is shown in Fig (2.3). PVG has the photo-voltaic array, the DC/DC and DC/AC converters and the associated controls as the main subsystems. A storage system generally does not exist in huge solar photovoltaic generator SPVG installations, except for small critical and sensitive loads of the power plant such as startup controls. However, in large-scale SPVGs, there are some exceptions of existing of integrated storage systems [19].

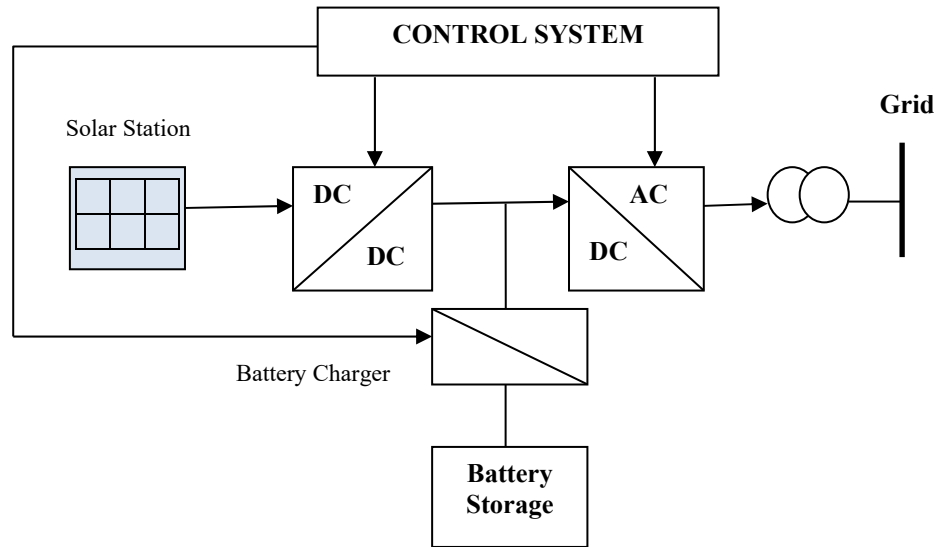


Figure 2.3: Grid connected photovoltaic generator.

A DC/DC converter which located at the output of the solar cells array regulates and boosts the voltage to the acceptable value. This converter is used to implement the process of tracking the maximum power point in SPVGs. For system stability analysis, the MPPT can be considered instantaneous because there are no dynamic devices contribute in this process [19,20].

2.2.2 Wind Turbines

Wind turbines are the most widely used SSG units which utilize the wind energy source. A wind turbine produces the mechanical energy by converting the kinetic energy of wind, and utilizing AC induction and synchronous types of generators, the electrical energy can be delivered. Wind turbines parts are a rotor, turbine blades, a shaft, a gear box, a coupling equipment, and a nacelle. The total efficiency of the wind turbine is about 20-40%, and its power capacity range between 300 to 7000 kW.

Four main types of the wind turbine are used in electric power utilities as shown in Figure (2.4) [10].

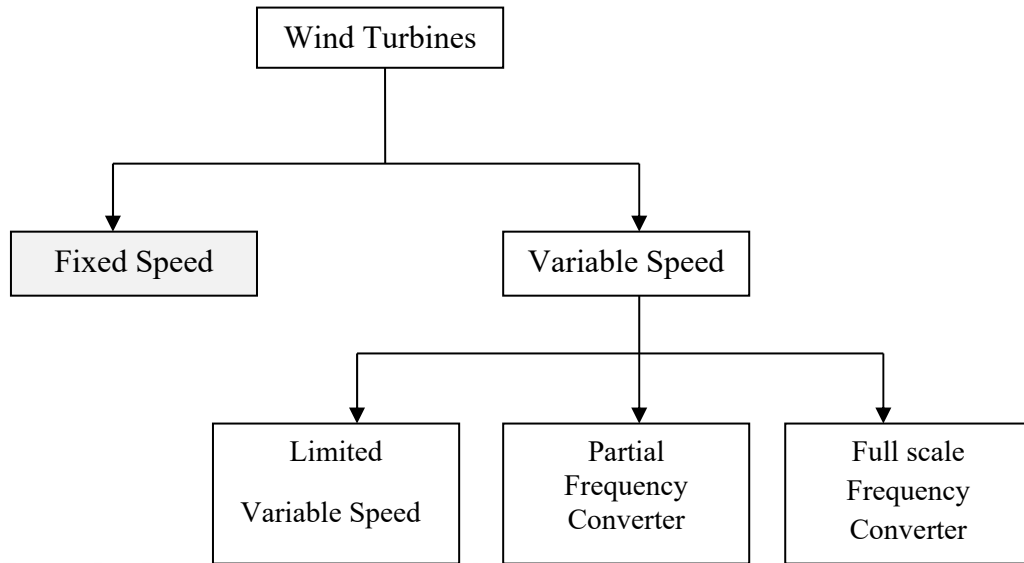


Figure 2.4: Types of wind turbines.

The presented work uses fixed speed wind turbine as one of SSG types that are integrated into DN.

Fixed Speed Induction Generator is widely used in wind turbines. It has many benefits such as mechanical simplicity, stiffness, and it has a low price. The induction generator has no permanent magnets and separate exciter, for this reason, the stator absorbs a reactive magnetizing current. Therefore it consumes reactive power. The network or a power electronic system device supplies the reactive power for induction generator [10].

The Squirrel Cage Induction Generator SCIG has been the suitable choice due to its mechanical plainness, low maintenance requirements, and high efficiency. The SCIG configuration is directly integrated into the grid.

The SCIG speed increases by only a few percent more than synchronous speed of the grid. Wind turbine type SCIG is connected with a reactive power compensation and soft –starter mechanism device because SCIGs absorb reactive power from the grid. SCIG has steep (vertical) torque speed characteristic, for this reason, fluctuations in wind power are transferred straight to the network.

In order to limit the inrush current, the SICG must be connected to the grid gradually. The inrush current could be up to 7-8 times the normal current, this current can cause excessive Voltage Disturbances. It is very stable and robust during normal operation when connected to a stiff AC network. If the load increases, the

slip of the induction generator increases. The main drawback is that the stator winding of the induction generator absorb reactive magnetizing current from the network, so the power factor in full is comparatively low. Definitely, low power factor generation not allowed due to its negative impact on voltage profile and grid stability.

By connecting capacitors in parallel to the generator low power factor could be compensated. Furthermore, in SCIG there is a unique link between the active and reactive power, terminal voltage, and rotor speed. This means in high winds the SCIG can deliver more active power on condition the generator consume more reactive power from the grid. This consumption is uncontrollable because it changes with wind conditions. Capacitor banks or modern converters should be used to reduce the reactive power consumption [10].

In the case of fault disturbance, SCIGs can cause voltage instability on the network. The wind turbine rotor might speed up due to slipping increase. For example, when a fault happens, this leads to imbalance state occur between electrical and mechanical torque. When the fault cleared, SCIG draws a lot of amount of reactive power from the grid, which effects on VS and voltage profile of the grid. (A simulation in case of fault has been presented in chapter four).

Voltage fluctuating in the grid caused by wind turbines power fluctuation during normal constant operation. The magnitude of the voltage fluctuation relies on the power factor of the SCIG and impedance phase angle of the network. The main reasons lead to Voltage Flicker are; the fast changes in the load or the switching turn on-off in the network (startup) or wind turbulence or fluctuations in the control systems.

Figure (2.5) describes the simplified equivalent circuit of fixed speed SCIG. Where x_1 and x_2 are the stator and rotor reactance respectively, x_m is the excitation reactance, r_2 is the rotor resistance. The stator resistance is neglected, s is the slip of the SCIG [21].

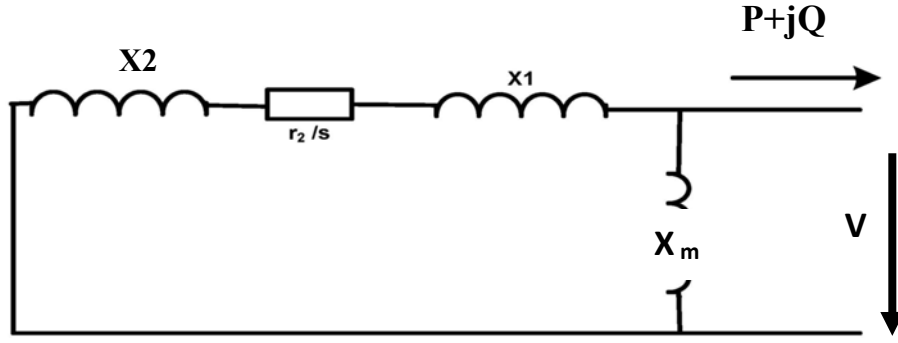


Figure 2.5: Fixed speed SCIG wind turbine equivalent circuit.

From the Figure (2.5), the following equations can be achieved:

$$V = \sqrt{\frac{-P(s^2 x^2 + r_2^2)}{r_2 s}},$$

$$Q = -\left(\frac{V^2}{X_m} + \frac{PX}{r_2} s\right) \quad (2)$$

$$x = x_1 + x_2$$

$$s = \frac{-V^2 r_2 + \sqrt{V^4 r_2 - 4P^2 x^2 r_2^2}}{2Px^2}$$

$$Q = -\frac{V^2}{x_m} + \frac{-V^2 + \sqrt{V^4 - 4P^2 x^2}}{2x} = f(V) \quad (3)$$

From equation (3), the active power P is a constant, and Q is a function of voltage, so, the P-bus power flow model of fixed speed SCIG bus is used [21].

2.2.3 Fuel Cells

It is an electrochemical equipment that converts the chemical energy of a gaseous fuel into electrical energy and thermal energy, with no combustion process [22]. FCs capacities diverse from 1 kW to a several MW according on the application. They have the ability to deliver power and heat at various scales and operates on different types of fuels such as fossil fuels, biomass based fuels, and renewable.

FCs have low emissions and high efficiencies but are likely too expensive for many applications. Currently, FCs are being utilized in many fields due to their high efficiency, high power quality, and environmental advantages. FC is an outstanding small size power generation units that convert Oxygen (air) and Hydrogen (fuel source) into the water and produces electricity.

Mainly, FC has two electrodes surrounding an electrolyte, where Hydrogen fuel injected into the Anode and the Air (Oxygen) passes through the Cathode and enters the cell. The electrical power is generated by controlling the movement of charged hydrogen and Oxygen atoms towards each other. The role of the electrolyte material is to provide a high resistance to the electrons and a very low resistance to the protons, show Figure (2.6).

The function of the electrolyte that is to allow the protons conduction and separate electrons by forcing them to pass to the other electrode via an external electrical circuit. This movement is controlled to produce regulated electrical power. The electrochemical process takes place without combustion, so the generation process is extremely efficient, clean and quiet [23].

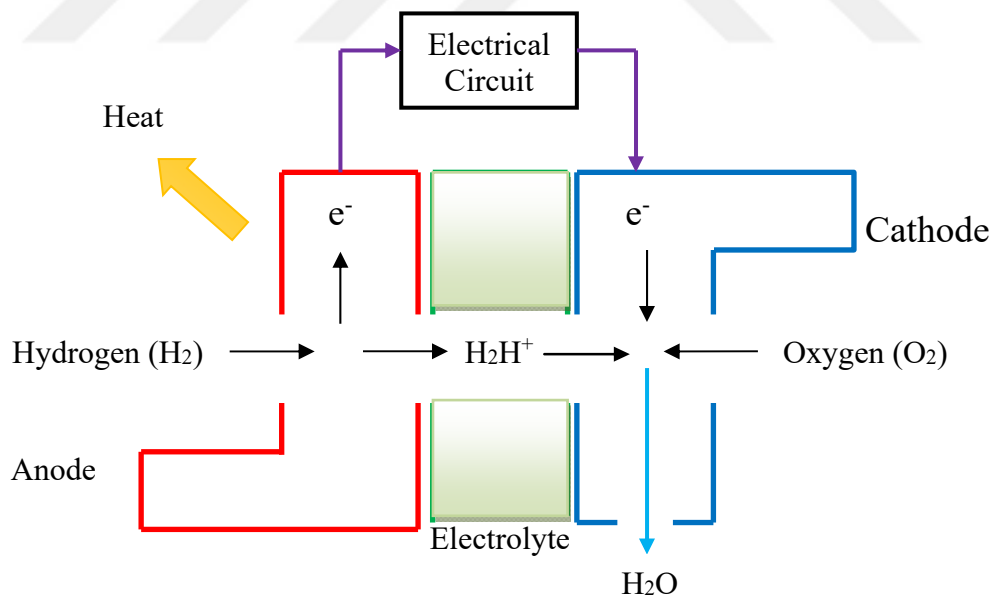


Figure 2.6: Operation principle of the fuel cell.

FCs Benefits are:

1. High efficiency operation: A practical electrical efficiency of FCs about 40% - 60% in the range, while the overall efficiency is 70% for small units and 75% for large units when using of both electrical and thermal power [28].

2. Flexibility of the fuel: The hydrogen which is used to generate electricity can be extracted from a different types of fuel sources like natural gas, ethanol, methanol, coal, and gasoline. Moreover, it can be use hydrogen from renewable sources such as biomass and through electrolysis from solar and wind energy.

3. Cogeneration ability: The thermal energy is produced besides the electrical energy. For instance, CHP system which participates in improving the unit efficiency.

4. Low emissions and Silent: FCs which operates on pure hydrogen emit only water vapor. On the other hand, FCs that use fuels such as natural gas, convert this hydrocarbon fuel to hydrogen and emit little air pollutants which still smaller than emissions from fuels that used in combustion systems. Furthermore, FCs are quiet units, this an important trait enables them to be installed near the customer loads.

5. Beneficial for the integration with renewable energy units: FCs can mitigate out the oscillations happening when PVG or wind turbine have been used in the system. Also, increase the power without any changing in the control system and the load demand will be covered more efficiently.

Fuel Cells drawbacks are extremely expensive and more works with researchers required in order to clear the reliability and withstand of high-temperature units [24].

Figure (2.7) shows the FC unit equivalent circuit and a DC/AC Pulse – Width Modulation Inverter (PWM) which converts the stack DC power to AC power [25,30].

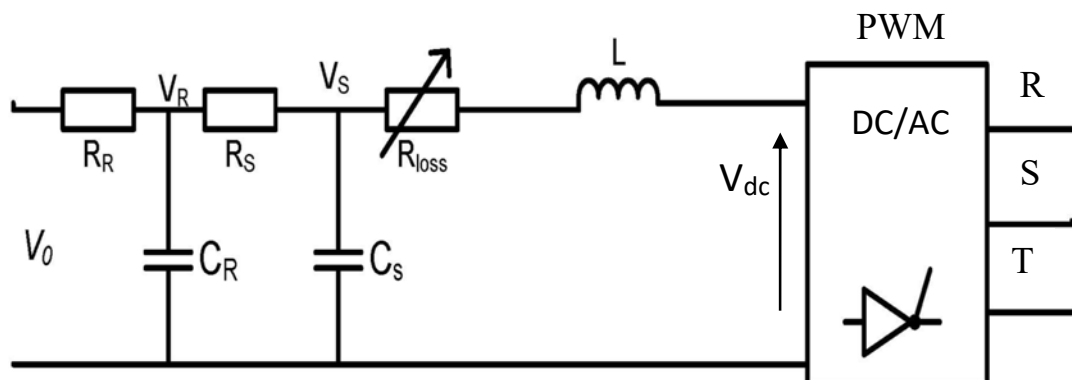


Figure 2.7: FC equivalent circuit.

Where:

V_0 : the open circuit cell potential

V_R : a reformer voltage signal

V_S : a stack voltage signal

R_{loss} : nonlinear – loss resistance introduced to account the voltage drop within the cell

L : a series inductor is connected due to the time constant of the current.

$$T_R = R_R \cdot C_R, \tau_S = R_S. \quad (4)$$

τ_R, τ_S : the reformer and the stack time constants

2.2.4 Micro – Turbines

MTs are excessive speed – small gas turbines which generate power in the range of 25 – 500 kW [27]. MTs are work on the same phenomenon of traditional gas turbines based on Brayton Cycle (constant pressure). MTs are used in many applications such as SSG units.

The rotor of the MTs is made to rotate at high speeds in the range of 50000 to 120000 rpm. The generator of MTs is a high – speed Permanent Magnet Synchronous Generator (PMSG) which used to generate AC power at a high frequency up to 10000 rad/s. This high frequency could be decreased, to match the synchronous frequency of the grid, using cycloconverters systems. A little amount of produced power in the generator is utilized for operating the air compressor [28].

The Advantages of MTs are:

1. Low installation costs, approximately 700\$ per kW
2. Maintenance costs are low, approximately 0.005\$ / KWh
3. Small in weight and size with the same capacity compared with other engines.
4. They can operate on a various types of fuels, such as natural gas, diesel, propane, ethanol, and gasoline
5. According to the conversion of fuel energy to the electricity, MTs have high efficiency reaching 25% - 30%. However, the overall efficiency level could be reaching 75% using the exhaust heat recovery process provided by recuperator.
6. They have a simple structure, so they are reliable and durable.

The cycloconverter in MTs is used to reduce and control the unit frequency and regulate the unit voltage. The rms output voltage on the grid side of the cycloconverter can be calculated as follows [29]:

$$U_{cy,o} = U_{cy,in} \sqrt{\frac{1}{\pi} \left(\pi - \alpha + \frac{\sin(2\alpha)}{2} \right)} \quad (5)$$

where:

$U_{cy,in}$: the rms input voltage of the cycloconverter

$U_{cy,o}$: the rms output voltage of the cycloconverter

α : firing angle

2.2.5 Reciprocating Internal Combustion Engine (ICE)

It is the most commonly used SSG technology and the least expensive among other units. It could be Reciprocating gas or Diesel engine. Diesel engines are commonly used and popular with end users for backup power and emergency backup due to their high level of pollutants emissions, this reason limited the number of unit running hours, approximately 150 hours per year. However, the natural gas engines emit fewer emissions, so they can be operated thousand hours each year [7].

The alternator could be a synchronous or induction generator. The synchronous type would be the most common choice for standby and network support application, while induction generator utilized for cogeneration application with capacity less than 300 KW because it is simpler than synchronous one to accomplish interconnection conditions to support islands.

2.2.6 Power Storage Units

The storage devices essentially are utilized to enhance stability and quality of power systems and used to backup fast load changes. There are a lot of storage devices, such as batteries, flywheels, super capacitor, and superconducting magnetic energy storage. They integrated into the power grid through power electronic converters [30].

2.3 Voltage Stability

The VS is an essential feature for power system quality, it means the capability of a power system to preserve stable and reliable voltages at all power lines and buses in the network after being applied to a contingency condition. If the network fails to compensate the increase of reactive power demand, then the voltage instability occurs [1].

2.3.1 Classification of the VS

Power system stability is the ability of the power system to stay in balance between the electricity supply and the demand under two main conditions, steady – state, and transient (disturbances).

The stability of the power system can be classified into VS, frequency stability, and rotor angle stability as shown in Figure (2.8) [2].

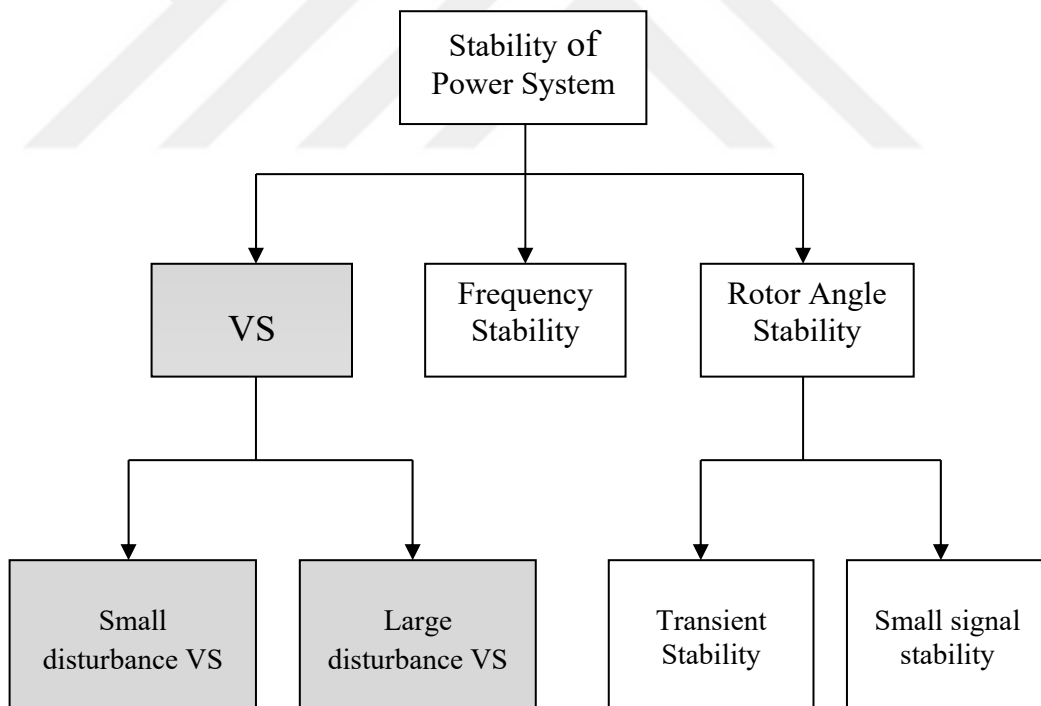


Figure 2.8: Classification of power system stability.

The large disturbance, such as faults, and large outages of the load or large step changes in the load are large contingencies. The large disturbance VS means the capability of the network to control the voltage after large contingencies occur. The

small disturbance VS is the ability of the system to control the voltage when small disturbances happen, such as loads variations [2].

2.3.2 Voltage Disturbances

Stable voltage means that the voltage is constant and sinusoidal, has a constant magnitude and frequency. VS analysis is performed to achieve perfect quality and reliability of any power system. The voltage disturbances, according to international standards [31], are divided in to:

Voltage unbalance is the voltage magnitude difference in (phase – phase) or (phase – neutral), or the phase angle between phases is not exactly 120° . It can be divided into steady – state unbalances and transient unbalances according to the cause and duration of the unbalance. The steady – state unbalance occur when the unequal distribution of loads is existed. Whereas, the common causes of transient unbalance are faults (line-to-ground) and fuse blown out in one of the phases in a capacitor bank [32].

Voltage Transients are sudden and fast changes of normal voltage which happen during (μs or ms) with very high magnitudes of voltage. The main reasons for transients are lightning, electrostatic discharges, and load switching. The excessive voltage during transients damages sensitive electronic devices and the insulation system that exposure to voltage transients on regular basis becomes weak and prone to insulation breakdown [33].

Voltage dip also knew voltage (sag) is a decrease in voltage magnitude for a short duration. According to European Standard [31], voltage dip is a rapid decrease in voltage to a level below 90 percent of its nominal value for no longer than a minute. The causes of voltage dips are short circuits faults, energizing of motor starting transformer, and arc furnaces. It affects on sensitive equipment such as measuring circuits and protection control device.

Voltage swell is an increase in voltage value for a short duration, this increase is about 110 % of the reference value. Voltage swell is considered as over voltage if the time duration is long, e.g. two minutes. It happens because of energizing of capacitor banks or disconnecting of a large load. The consequences of voltage swell are the same as for those voltage dips [32].

Voltage flicker is small periodic voltage amplitude changes occurring at frequencies in the range of 0.5 Hz and 25 Hz, that cause visual disturbance and variations in lighting levels. It is caused by large fluctuating loads such as electric welding, large transformer tap changer or fast change in power level. Figure (2.19) shows voltage flicker [33].

Harmonic distortion of the voltage is a periodic variation of the ideal waveform, occurring when frequencies of the multiple integers are added to the essential frequency of the voltage waveform. It can be caused by non-linear loads such as power electronic devices, rectifiers, inverters. Also, it causes heating of equipment, increasing line losses, and interfaces with measuring and protection systems [33].

2.4 Impacts of the SSG Units on Voltage Profile and Voltage Stability

Remaining the voltage within acceptable limits along all load feeders in the DN is crucial to prevent unsuitable operation of the power system and customer appliances. A common way in controlling the voltages is based on tap – changing transformers to regulate the source voltages at substations [34]. Furthermore, VAR compensators, synchronous condensers, or static or switched capacitors can be used on feeders to control and compensate the reactive power [35].

Supplying additional amount of power using SSG units in DN can effectively enhance and support feeders voltages if these units are optimally integrated with the network. This can be done by controlling the reactive power using power factor converters depending on voltage levels on local feeders [34].

In RDN, the measured loads on the feeders will be less than actual values because of the on-site generated power. For this reason, the voltage regulators will not precisely measure real feeder demands. As a result, the tap changing transformers will not be optimal for the influential regulation of the voltages at all feeder buses [34,35].

The integration of SSG units reduces the gap between maximum and minimum values of buses voltages. Whereas, without these units, the voltages decrease with the distance of the bus from the central power source.

In DN, voltage instability occurs either from the gradual collapse or increasing of voltages of network buses, which lead to loss of some loads or lines. Also, if the

loads consume reactive power much more than the capability of the lines and generators, then the voltage instability takes place.

Steady – state voltage fluctuations at the load terminals in DN can be reduced by integration SSG units near to them. Moreover, all SSG units have conventional reactive power controllers and regulators to control their performance, so some enhancements are achieved in the performance of the loads especially during disturbances or short circuit faults. Also, high-level SSG units integration increases the voltage damping ratio when the reactive – load switching happen in the network. Optimum SSG unit capacity and location in a DN have a significant impact to develop VSM using an optimization technique that determines the most sensitive voltage buses in the network to place the SSG unit [4].

Although the integration of the SSG units has many advantages, they increase the complexity of control and protection strategies of the network. In some cases, the directions of active and reactive power of SSG units may be reversed and contracts the original ones. Therefore, this contraction affects the stability of the network. Also, harmonic resonance due to the high penetration of the SSG units effects on power quality [36].

CHAPTER THREE

MODELING AND ANALYSIS USING MATLAB / PSAT

3.1 Introduction

This chapter concentrates on the modeling of different types of SSG units integrated in 33 – bus RDN using MATLAB / PSAT Toolbox (Power System Analysis Toolbox). Also, this chapter focuses on VS analysis techniques which are used to determine the VS margins of the proposed DN which integrated by different types of SSG units during steady – state and contingency conditions [37].

The VS analysis principle is based on power flow analysis, continuation power flow (CPF), time domain simulation, and frequency domain simulation (small signal stability analysis). Different types of SSG units are integrated into network such as a PVG, a Fuel cell, a wind turbine Induction generator, and a synchronous generator. All the SSG units will be connected individually at an optimum location in the network with optimum capacity before applying VS analysis on the model.

3.2 An Open source Power System Analysis Toolbox (PSAT)

It is a MATLAB depended software program for modeling and analysis of medium and small scale electric power networks. Power flow, continuation power flow, small signal stability analysis, and time domain simulation, and many static and dynamic models such as synchronous and induction machines, loads, FACTS, and several controls models are available in PSAT. The toolbox is supported with a graphical user interface and a Simulink (based on) one – line network editor. Also, it is enforced with the most total group of algorithms which belong to static and dynamic analyses among other power system software programs which used in MATLAB. Figure (3.1) shows the main graphical user interface of PSAT [37].

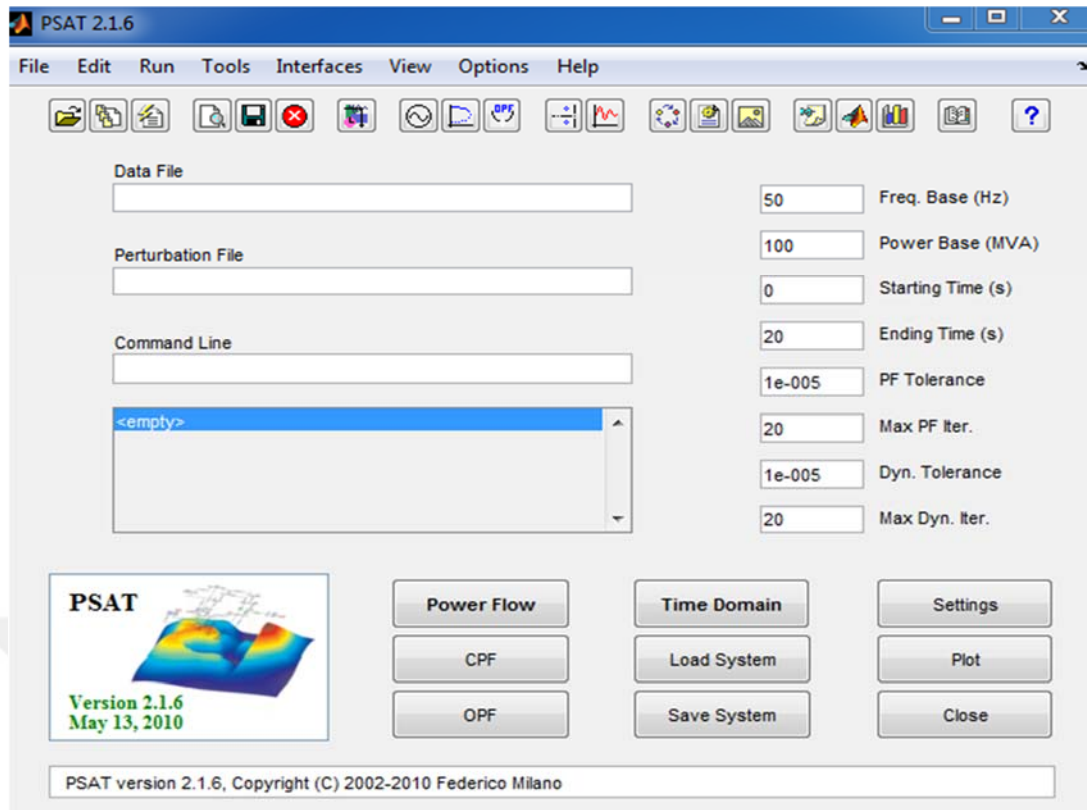


Figure 3.1: PSAT main graphical user interface.

3.3 33-bus Distribution Network Model

The 33-bus network is used and modeled using PSAT. This model has one slack bus (reference bus), 32 transmission lines, and 32 (P-Q) constant loads [38]. The rated voltage for the system is (12.66 kV) and the rated power is (1 MVA). All parameters values for the system are in per units. The lines and loads data for the system are given in Appendix A. Figure (3.2) shows the 33-bus radial distribution network model.

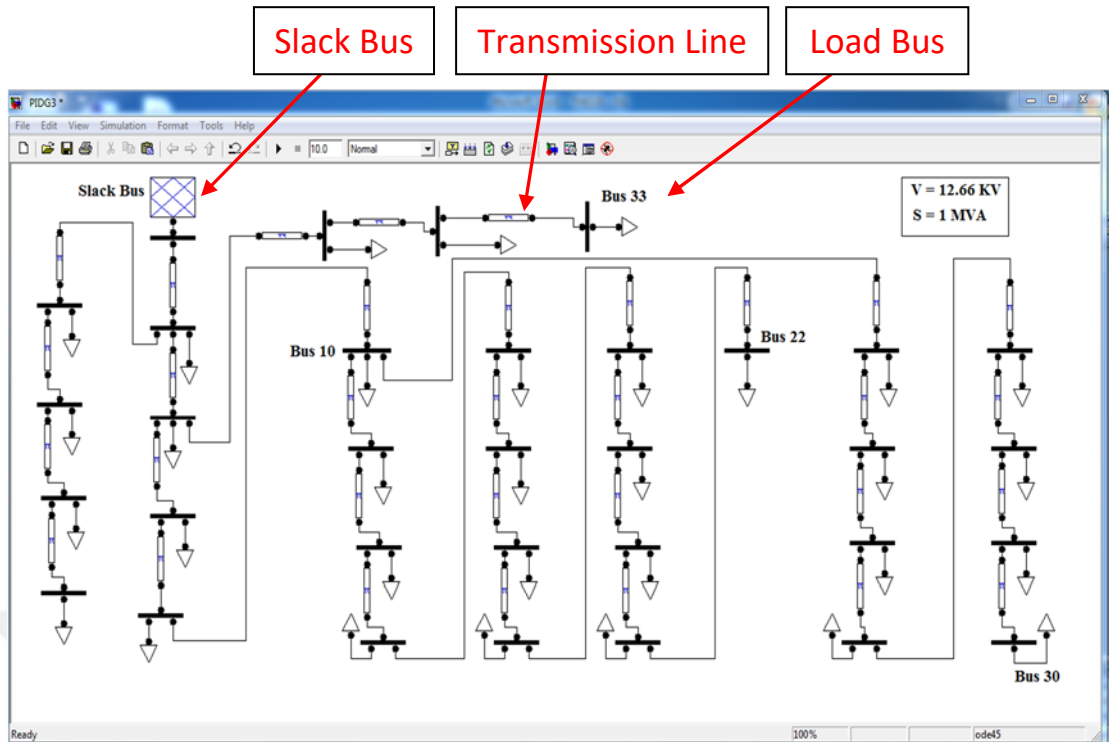


Figure 3.2: 33-bus radial distribution network model.

3.3.1 Slack and Load Buses Model

Conventional power flow analysis for DN utilizes a distributed slack bus, which generally represents a substation for distribution systems (It is an equivalent model of a big system) [39]. There are two familiar definitions about the slack bus, one is the slack bus represents the angle reference bus ($V - \Theta$) bus. The other definition is the bus that balances the active power (p) in the system [40].

The bus that connected with different types of loads known as a load bus. In presented work, constant loads (PQ) are used. The model identification of slack and load buses is illustrated in Table (3.1).

Table 3.1: Model Identification of the Slack and Load buses.

Buses	Rated S(MVA)	Rated V(KV)	V(p.u.)	Θ (deg.)	Input	Output
Slack	1	12.66	1	0	–	1
Load	–	12.66	Calculated	Calculated	Optional	Optional

3.3.2 Transmission Line Model

Figure (3.3) shows the transmission line lumped model.

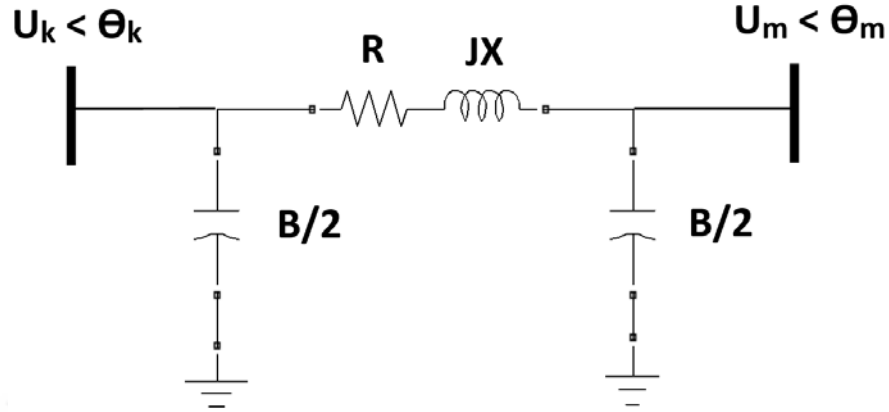


Figure 3.3: Transmission line π circuit.

The line power flow equations are as follows [41]:

$$P_k = U_k^2(g_{km} + g_{k0}) - U_k U_m [g_{km} \cos(\theta_k - \theta_m) + b_{km} \sin(\theta_k - \theta_m)]$$

$$Q_k = -U_k^2(b_{km} + b_{k0}) - U_k U_m [g_{km} \sin(\theta_k - \theta_m) - b_{km} \cos(\theta_k - \theta_m)]$$

$$P_m = U_m^2(g_{km} + g_{m0}) - U_k U_m [g_{km} \cos(\theta_k - \theta_m) - b_{km} \sin(\theta_k - \theta_m)]$$

$$Q_m = -U_m^2(b_{km} + b_{m0}) + U_k U_m [g_{km} \sin(\theta_k - \theta_m) + b_{km} \cos(\theta_k - \theta_m)]$$

where:

U : is the bus voltage.

$$y = \frac{1}{Z} = \frac{1}{R + jX} = \left[\frac{1}{R + jX} \times \frac{R - jX}{R - jX} \right] = \frac{R - jX}{R^2 + X^2}$$

$$= \frac{R}{R^2 + X^2} - \frac{jX}{R^2 + X^2} = g + jb, \text{ We see that:}$$

$$g = \frac{R}{R^2 + X^2} \text{ and } b = \frac{-X}{R^2 + X^2} \quad (3.1)$$

3.3.3 PQ Load Model

The model of PQ loads is constant active and reactive powers:

$$P \bullet = -P_L \quad (3.2)$$

$$Q \bullet = -Q_L$$

PQ loads are altered into fixed impedances If a voltage limit is transgressed, as follow:

$$P = -PV^2 / V_{lim}^2 \quad (3.3)$$

$$Q = -QV^2 / V_{lim}^2$$

3.4 PV Generator Model

This model fixes The voltage amplitude and injected power at the bus are constant where it is connected according to set values, as follows

$$P = P_g \quad (3.4)$$

$$Q = V_0$$

This model represents a generator with voltage control operation mode [53]. In proposed case a distributed slack bus model was used, the active power equation becomes:

$$P = (1 + \gamma k_G)P_g \quad (3.5)$$

where:

γ : The loss participation factor, (1) for the slack bus and (0) for SSG units

k_G : Scalar variable of the distributed slack bus

3.5 PQ Generator Model

Constant active and reactive powers were used in this model, as follows:

$$P^\bullet = P_g \quad (3.6)$$

$$Q^\bullet = Q_g$$

$$\cos \theta = \frac{P_g}{\sqrt{P_g^2 + Q_g^2}}$$

This model represents a generator with a power factor control operation mode [53].

3.6 Photovoltaic Generator Model

The photovoltaic generator can be modeled according to the equivalent circuit of photovoltaic grid connected circuit as shown in Figure (3.4):

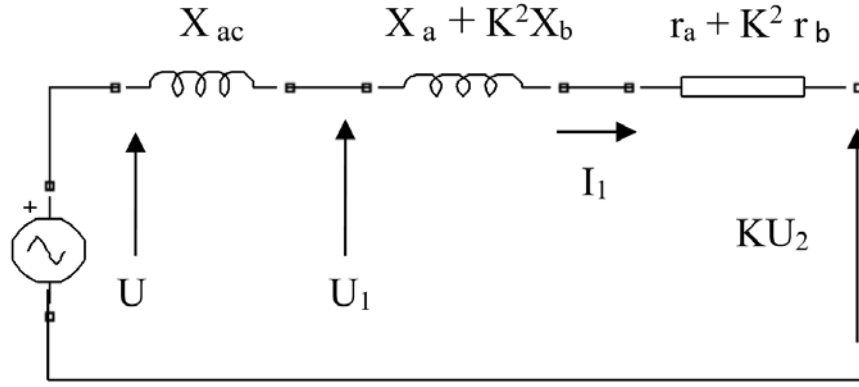


Figure 3.4: Equivalent circuit of photovoltaic grid-connected system.

The voltage equations can be obtained [42]:

$$U = KU_2 + I_1 [(r_a + K^2 r_b) + j(X_{ac} + X_a + K^2 X_b)] \quad (3.7)$$

$$U_1 = KU_2 + I_1 [(r_a + K^2 r_b) + j(X_a + K^2 X_b)]$$

where:

U : Output voltage for PV array inverter (v)

U_1 : Output voltage for inverter filter (v)

U_2 : Transformer secondary side voltage (v)

K : Transformer ratio, ($K < 1$)

I_1 : Inverter output current (A)

r_a : Primary side parasitic resistance (Ω)

r_b : Secondary parasitic resistance (Ω)

X_a : Primary side drain (Ω)

X_b : Secondary side drain (Ω)

X_{ac} : Inverter AC side filter reactance (Ω)

The photovoltaic generator is modeled in this work according to the operation modes, once as a PV generator and second as a PQ generator [42,53,54].

3.7 Fuel Cell Model

Fuel cell generator must be interfaced with the DN via a power converter because the fuel cell generates DC power that should be converted to AC. Forced – commutated Voltage Source Inverter (VSI) is used for interfacing a fuel cell unit [43]. Figure (3.5) shows a one-line diagram of the fuel cell generator with its inverter unit (VSI).

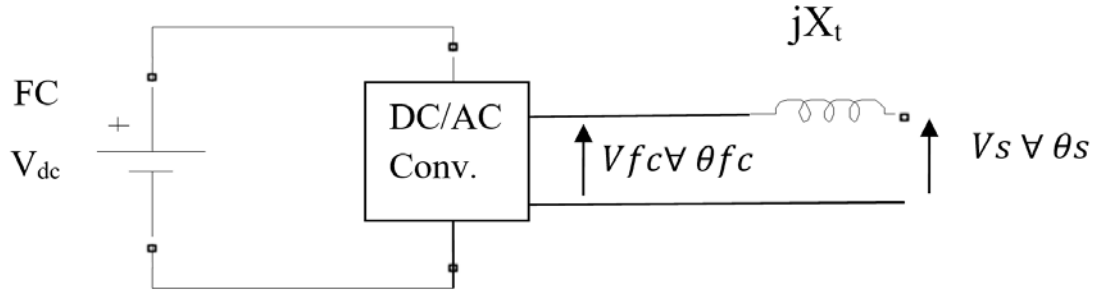


Figure 3.5: Fuel cell generator with (VSI) Inverter.

The active and reactive power of fuel cell generator are given by following equations:

$$P_s = \frac{V_{fc} V_s}{X_t} \sin(\theta_{fc} - \theta_s) \quad (3.8)$$

$$Q_s = \frac{V_{fc} V_s}{X_t} \cos(\theta_{fc} - \theta_s) - \frac{V_s^2}{x_t}$$

where:

V_{fc} : The AC voltage of the inverter

V_s : Transformer secondary winding voltage

X_t : The leakage reactance of the transformer

3.8 Constant Speed SCIG Wind Turbine Model

The equivalent electrical circuit of the constant speed squirrel cage induction generator is similar to the squirrel cage induction motor, illustrated in Figure (3.6), the difference is that the current in the induction generator is positive and injected into grid, since the slip of the induction generator is negative, which means that the rotor speed of the generator is slightly greater than the flux speed of the stator.

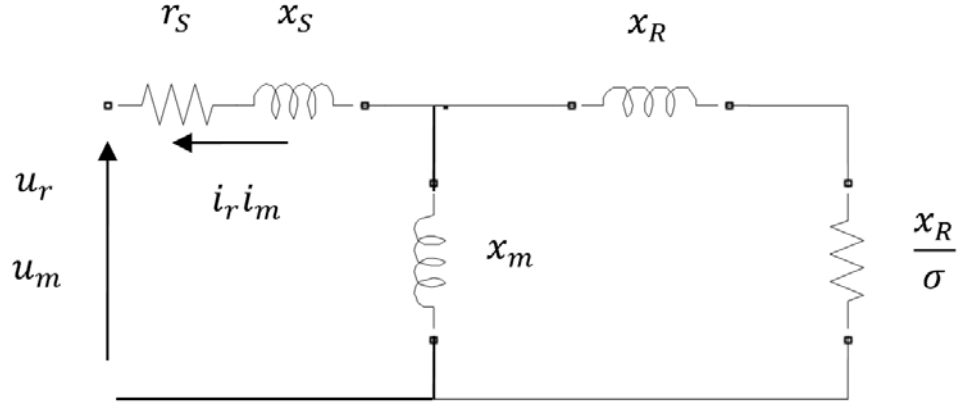


Figure 3.6: Squirrel cage induction generator equivalent circuit.

The real (r) and imaginary (m) axis are represent the equation form as a function of network reference angle. The relationship between the grid and the voltages of the stator machines is shown as follows:

$$u_r = U \sin(-\theta) \quad (3.9)$$

$$u_m = U \cos(\theta)$$

And the power equations are:

$$P = u_r i_r + u_m i_m \quad (3.10)$$

$$Q = u_m i_r - u_r i_m + b_c (u_r^2 + u_m^2)$$

where b_c is the capacitor conductance of the SCIG wind turbine [41].

3.9 Synchronous Generator Model

The relationship between the machine voltage the network phase angles is as follows:

$$u_d = U \sin(\delta - \theta) \quad (3.11)$$

$$u_q = U \cos(\delta - \theta)$$

Where δ is the load angle of the machine.

The active and reactive powers of the generator are defined as follows:

$$P = u_d i_d + u_q i_q \quad (3.12)$$

$$Q = u_q i_d - u_d i_q$$

Where i_d, i_q are the currents of d and q axis

3.10 Voltage Stability Analysis Methods

The VS of the proposed models, (in chapter four), was examined using three different techniques which are available in PSAT. Basically, these three methods are based on power flow solver which is available in PSAT too. The voltage analyses are; Static, Dynamic, and Proximity to voltage instability.

3.10.1 Power Flow Solver

It is the solution of nonlinear power flow equations which are in the form:

$$f^*(x, y) = 0 \quad (3.15)$$

$$g^*(x, y) = 0$$

Where:

x : Represents the state variables, which are active (P) and reactive (Q) powers at the network buses.

y : represents the algebraic variables, such as voltage amplitude and phases θ at the grid buses, generator field and AVR reference voltages.

f : The differential equations.

g : The algebraic equations.

Newton-Raphson technique [44] is implemented to solve the power flow equations of the proposed models. By utilizing the Jacobian matrix of differential and algebraic equations (3.16):

$$[J] = \begin{bmatrix} F_x^i & -F_y^i \\ G_x^i & G_y^i \end{bmatrix} \quad (3.16)$$

Where $F_x = \frac{df}{dx}$, $F_y = \frac{df}{dy}$, $G_x = \frac{dg}{dx}$, $G_y = \frac{dg}{dy}$

$i = 0-1-2-3-4 \dots i+ n$ (number of iteration)

So, the N-R method updates the Jacobian matrix at each iteration as follows:

$$\begin{bmatrix} \Delta x^i \\ \Delta y^i \end{bmatrix} = - [J]^{-1} \begin{bmatrix} f^i \\ g^i \end{bmatrix} \quad (3.17)$$

$$\begin{bmatrix} x^{i+1} \\ y^{i+1} \end{bmatrix} = \begin{bmatrix} x^i \\ y^i \end{bmatrix} + \begin{bmatrix} \Delta x^i \\ \Delta y^i \end{bmatrix}$$

The iteration routine will stop if one of the two conditions occurs; The increments variables Δx and Δy are less than the value of a given tolerance ϵ_0 in (PSAT setting) or the iteration number is greater than a setting limit ($i > i_{max}$).

3.10.2 Static Analysis Method

It depends on the Lambda-Voltage (λ -V) curve to find out the voltage stability of network buses. λ -V curves for all buses could be plotted using Continuation Power Flow (CPF) technique which is available in PSAT by executing a large number of power flows [41].

The nonlinear differential equations of any power system are presented as:

$$\dot{x} = f(x, \lambda) \quad (3.18)$$

where

$x \in R^n$ a state vector which represents the bus voltage amplitude (V) and angles (δ).

$\lambda \in R^m$ a parameter vector which represents the active (P) and reactive (Q) required powers at each load bus.

The λ varies due to variation in the load, so the power flow solution varies at each value of λ [45]. The power flow for the power network is represented by;

$$0 = f(x, \lambda) \quad (3.19)$$

The equation (3.19) gives two equilibrium solutions; the first solution has a high voltage value, whereas the other has a low voltage value. The solution with the higher voltage value is the stable solution.

The λ -V curve is formed by increasing the loading at the bus, the higher voltage solution values decrease and the lower voltage values increase until they come together into a critical loading power point (λ_{max}) which determines the voltage stability margin boundary [46,47]. These solution points represent the λ -V curve (nose curve). Figure (3.8) illustrates the λ -V curve [54].

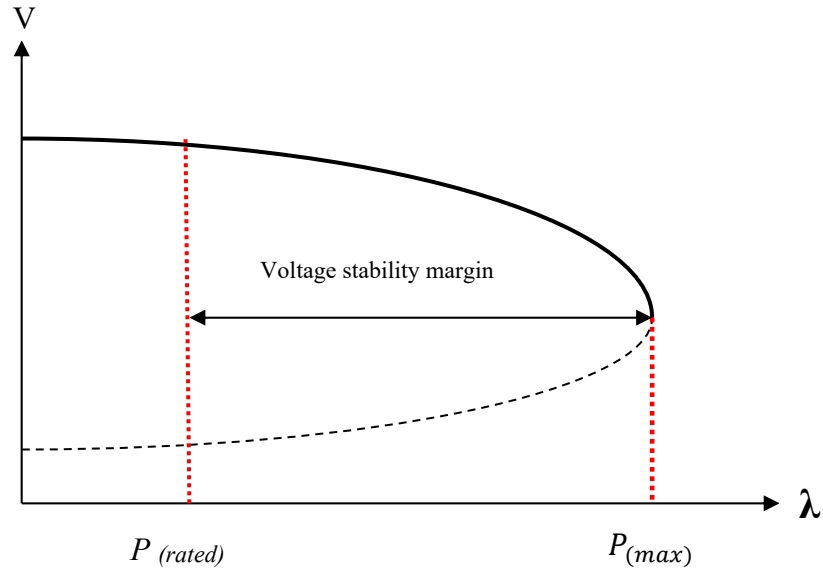


Figure 3.7: λ -V curve.

$$\lambda_{(max)} = \frac{P_{(max)}}{P_{(rated)}}, \lambda > 1 \quad (3.20)$$

Also (V-Q) sensitivity analysis is used to determine the voltage stability, but not tackled in presented work.

3.10.3 Dynamic Analysis Method

Dynamic analysis demonstrates the actual performance of the power system during normal control actions and disturbances conditions. It can be done in a time domain simulation using Trapezoidal integration method [49]. The power system can be introduced by first order differential and algebraic equations as follows:

$$\dot{X} = f(x, U) \quad (3.21)$$

$$J(x, V) = Y_N U$$

where:

X : System state vector

U : Bus voltage vector

J : Current injection vector

Y_N : Network node admittance matrix

These equations can be solved using Trapezoidal numerical integration method. For total time t and a time step Δt , the equation (3.21) in terms of time can be written as follows:

$$0 = f_n(x(t + \Delta t), U(t + \Delta t), f(t)) \quad (3.22)$$

$$0 = I(x(t + \Delta t), U(t + \Delta t))$$

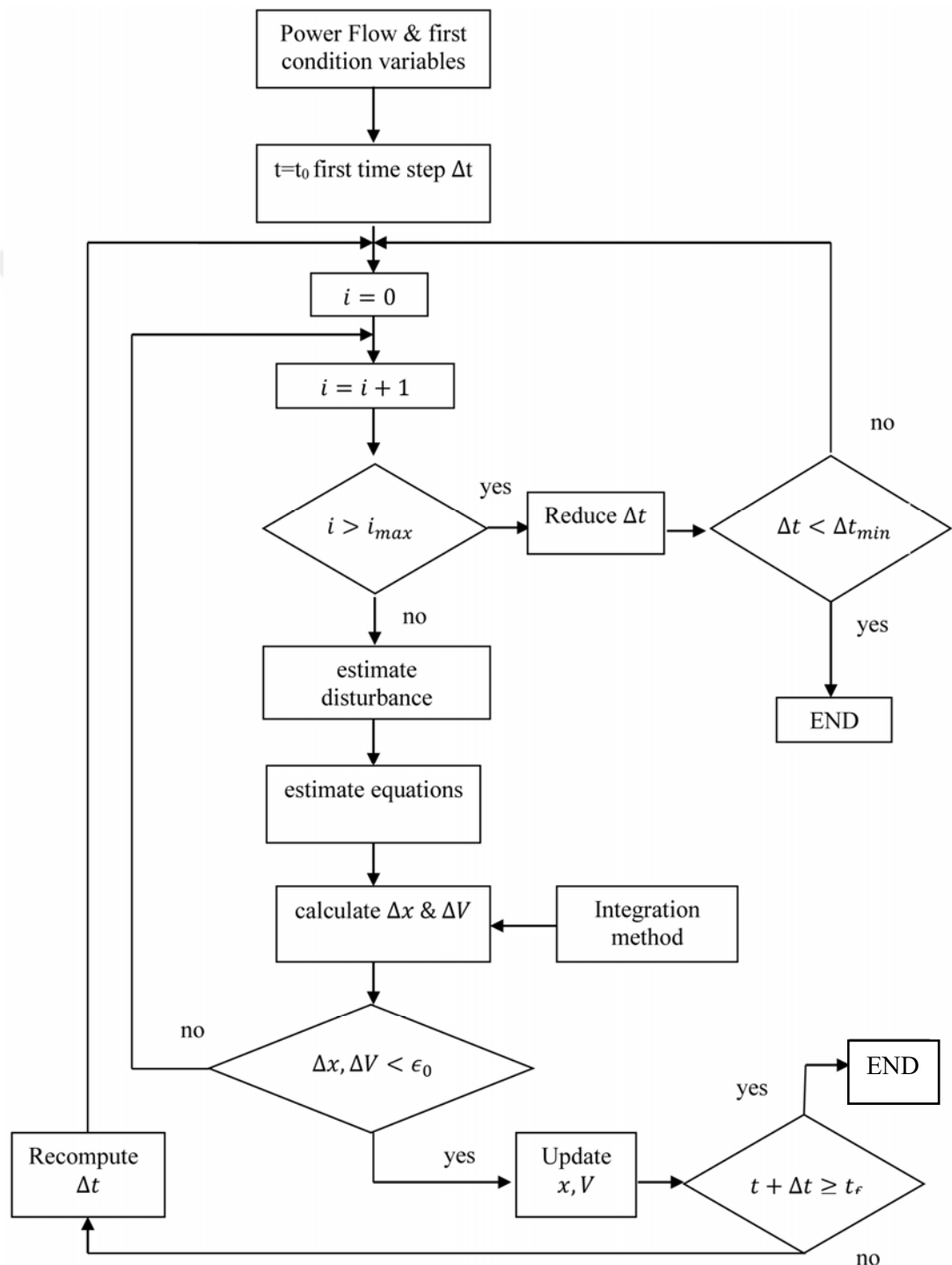


Figure 3.8: Time domain integration block diagram.

The equations (3.22) are nonlinear and can be solved by means of a Newton-Raphson method. However, in this case, the time step Δt is reduced at each repeated iteration which computes the updated state and algebraic variables $\Delta x^i, \Delta V^i$. Figure (3.9) shows the time domain integration block diagram.

3.10.4 Proximity to Voltage Instability Analysis Method

The static analysis cannot illustrate the control action and the interaction impact between the integrated SSG unit and distribution network during operation. This issue can be determined using small-signal stability analysis which is achieved in the frequency domain using Eigenvalue analysis [50].

It is possible to calculate and visualize the Eigenvalues of the network after solving the power flow problem and computing the State Matrix A_{St} of the network by multiplying all elements of the Jacobian matrix (3.16) as follows [41]:

$$A_{St} = F_x - F_y G_y^{-1} G_x \quad (3.23)$$

The Eigenvalues are consist of real parts and imaginary parts which represent the (Poles) of the system. The real parts locations in the S domain can determine if the system is stable or unstable, all of them should be less than zero (negative) when the system is stable. Whereas in Z domain, all the poles must be inside the circle in the stable system [51,52].

Figure (3.10) shows the system poles locations in the S domain and their oscillatory conditions.

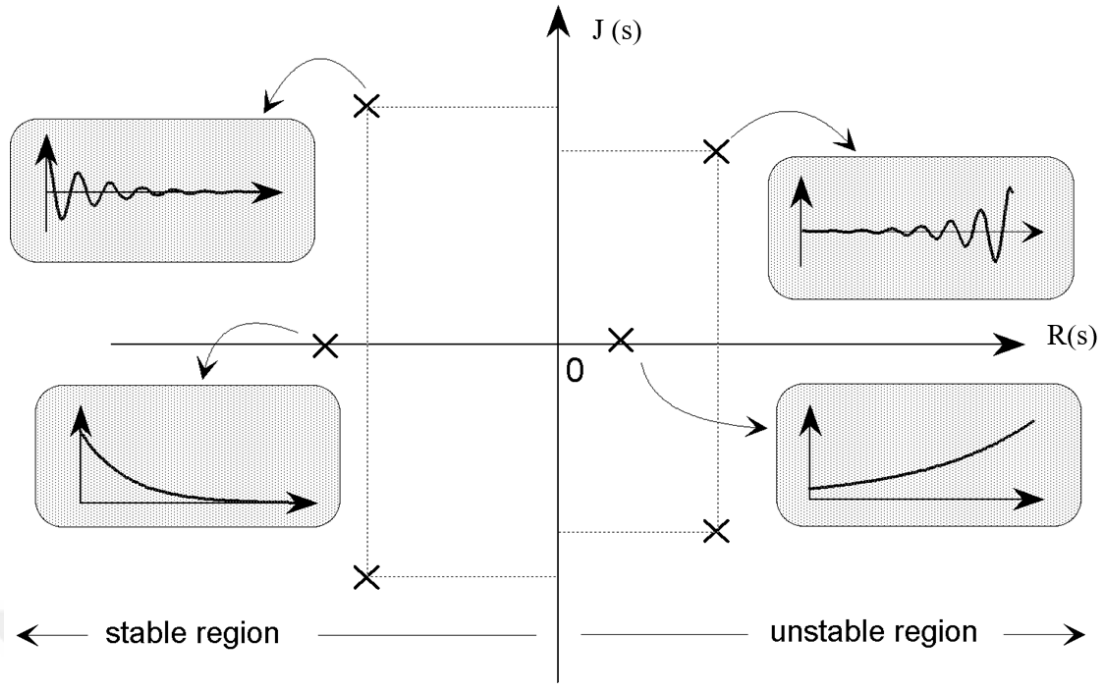


Figure 3.9: A System poles locations in the S domain.

3.11 Optimum Location and Size of SSG Units

The SSG capacity and location were optimized in order to obtain precise analysis results with minimum active power losses in the network. A lot of techniques and researches were implemented to determine the optimum capacity and location of integrated SSG units in the DN.

In presented work, the Loss Sensitivity Factor (LSF) technique was applied [55]. The aim of this method is to specify the optimum location of SSG unit in the network and optimum capacity increment which based on minimization of active power loss. LSF for any candidate bus (i) that connected with (SSG_i) unit can be determined as follows:

$$LSF_i = \frac{\Delta P_{loss}}{\Delta P_i} = \frac{P_{loss}^i - P_{loss}^{base}}{P_{SSG,i}^{inc}} \quad (3.24)$$

Where

P_{loss}^{base} : The base case total system loss (without SSG)

$P_{SSG,i}^{inc}$: SSG capacity increment which connected to i^{th} bus

P_{loss}^i : The system loss with increment in SSG capacity

If the LSF is negative value the system loss is reduced, else, if the LSF is positive value the SSG integration at the bus (i) increases the system loss, otherwise, the SSG injection has no effect.



CHAPTER FOUR

SIMULATION AND RESULTS

4.1 Introduction

This chapter presents two main aspects; the first one is the simulation of RDN without SSG integration (Base Case) and with the integration of different types of SSG units individually with optimum capacity and location. The SSG units are; Static (photovoltaic and Fuel Cells generators) and dynamic (Synchronous and Induction generators).

The second aspect is applying three types of VS analysis (Static, Dynamic, and Small signal stability Analysis) on simulated models with integration each type of the proposed SSG units individually. Moreover, this chapter discusses the analysis results to evaluate the impact of different SSG units on voltage stability and loadability of the RDN in order to determine the best SSG unit type that improves the VS margin of the network.

All the simulated models and analysis had been performed using Power System Analysis Toolbox (PSAT) / MATLAB program which supports the Graphic User Interface (GUI). All the analysis (static, dynamic, and small-signal stability) are based on Power Flow Analysis Newton-Raphson method. Figure (4.1) shows the block diagram of the main steps of the proposed work.

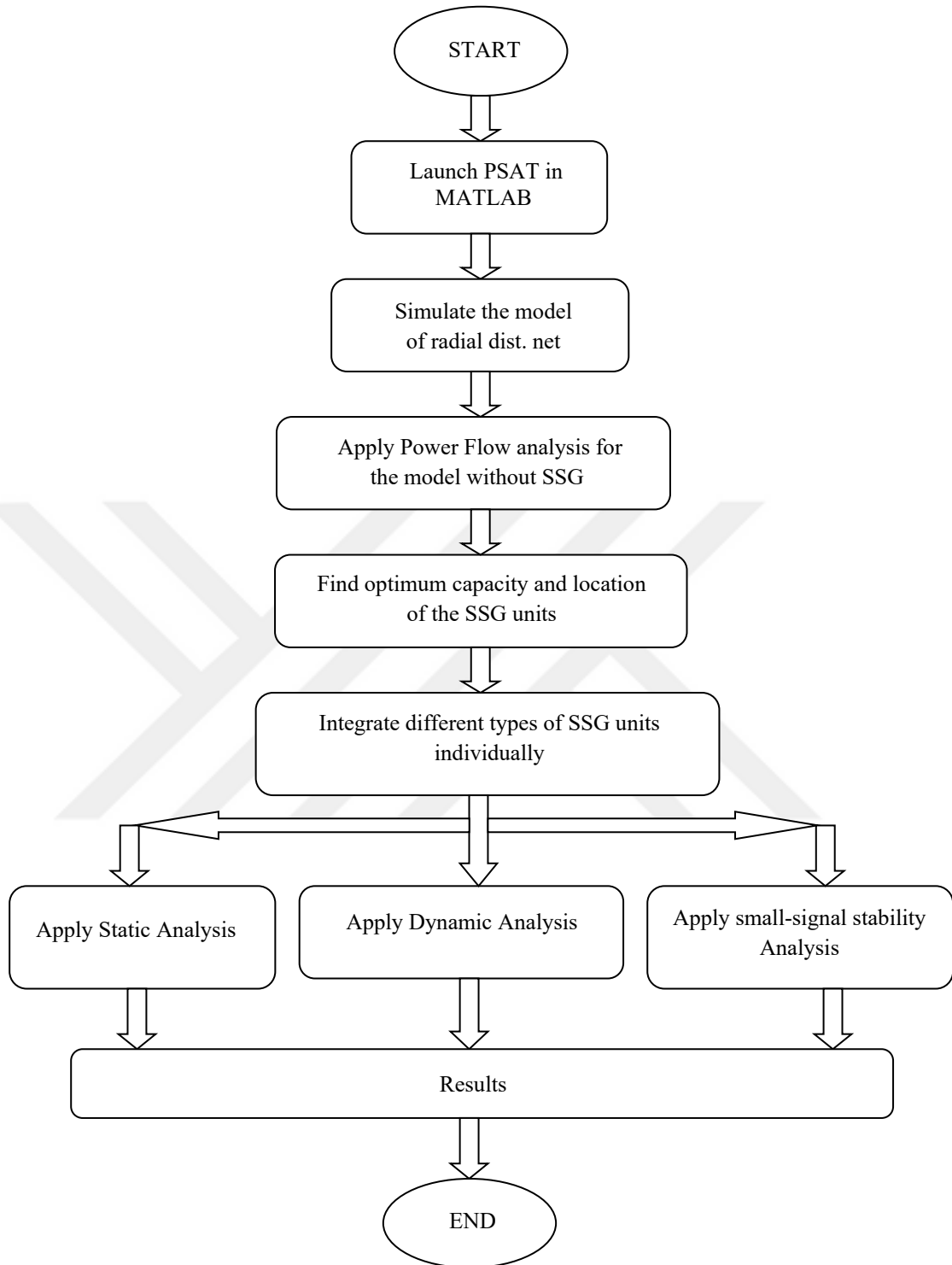


Figure 4.1: Main steps of the proposed work.

4.2 Distribution Network Model Simulation

The 33-bus RDN was used to examine the VS margin after integration of different types of SSG units. The radial network is modeled and simulated using

PSAT in MATLAB. The model has one Slack bus, 32 load buses, and 32 lines. The model has base apparent power 1MVA (1p.u.), base voltage 12.66 kV (1 p.u.), and total constant P-Q loads 3.7 MW and 2.3 MVAR respectively.

Appendix (A) shows the lines and loads data of the network. Figure (4.2) illustrates the base case (without SSG units) of single line network which modeled using PSAT.

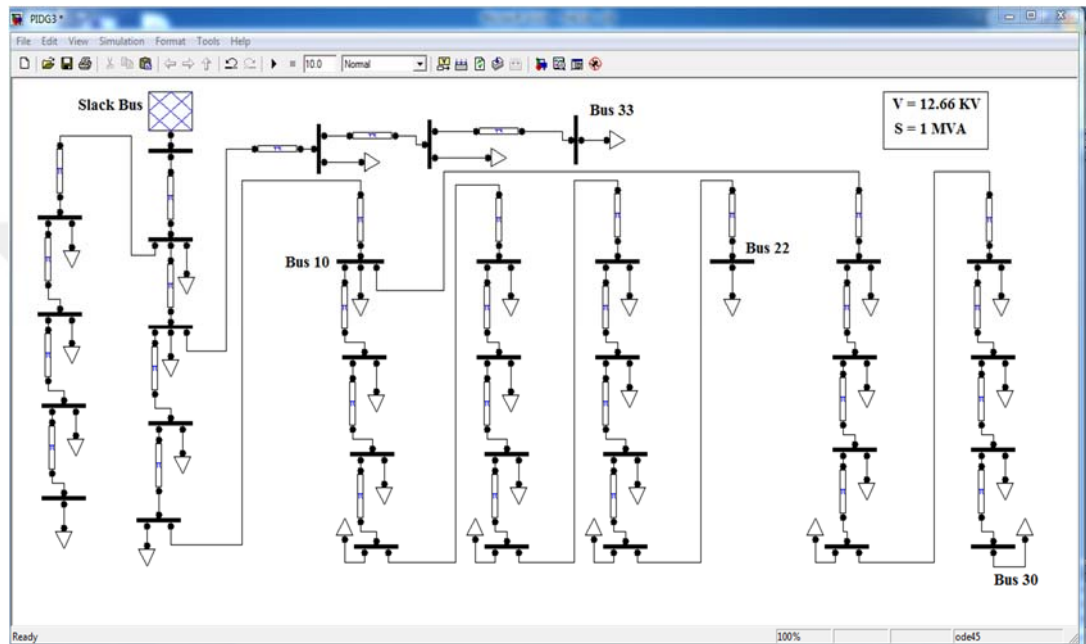


Figure 4.2: Single line Model of 33-bus radial network (base case).

4.3 Network Power Flow Analysis (without SSG unit)

The power flow results of the base case model are illustrated in Appendix (B.1) as a text file. N-R method is used to perform this issue in PSAT. The power flow analysis is mandatory before each analysis type in PSAT. In this work, the ‘Total Generation’ means the total active and reactive powers that are supplied from utility to the distribution DN. The (slack bus or substation) represents the utility generation.

Table (4.1) shows the global summary report of power flow analysis of RDN without SSG units (base case).

Table 4.1: Summary report of power flow of the network (base case).

Total Generation	Network Total load	Network Total losses
3.9 MW	3.7 MW	0.169 MW
2.4 MVAR	2.3 MVAR	0.105 MVAR

The static analysis of the model was implemented using continuation power flow (CPF) analysis technique. Appendix (B.2) shows the CPF report. The main objective of utilizing CPF analysis is to draw the λ -V curves for the load buses. These λ -V curves show the VS margins and maximum loading points of buses. These points determine the maximum loading parameter λ_{\max} which represents the collapse point of the buses voltages. Table (4.2) shows the results of CPF summary report of the RDN (base case).

Table 4.2: Summary report of CPF of the network (base case).

Total Generation	Network Total load	Network Total losses
21.8 MW	13.5 MW	8.324 MW
14 MVAR	8.3 MVAR	5.714 MVAR

Figure (4.3) depicts the network (base case) CPF visualization using Graphic User Interface GUI.

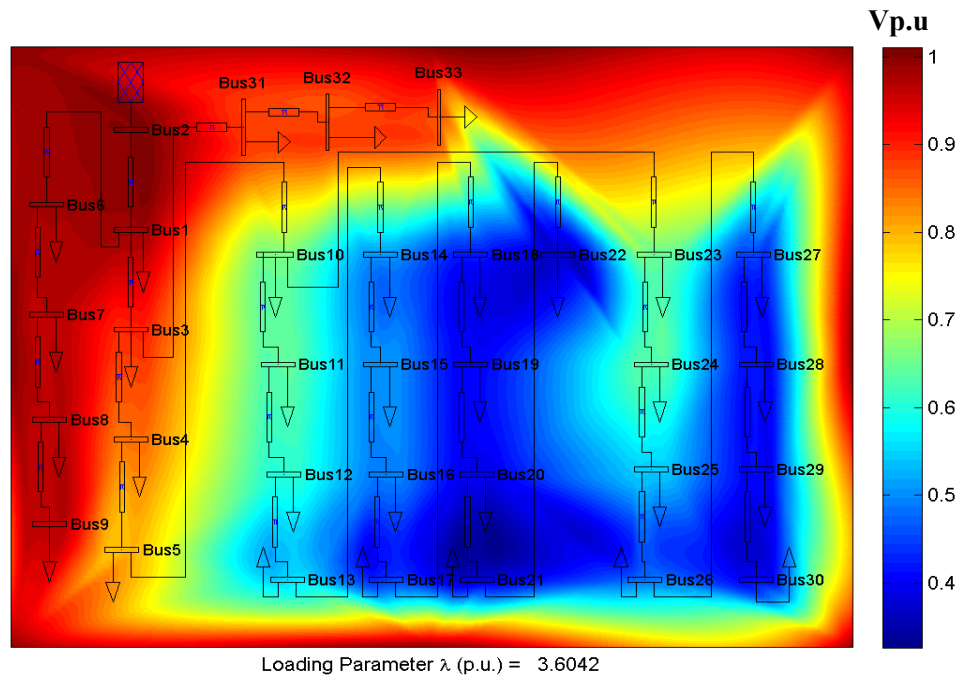


Figure 4.3: GUI of CPF network visualization.

From the figure above it is clear that the buses 22 and 30 have the lowest voltages profiles among other buses in the system, 0.46 p.u and 0.49 p.u respectively, due to their distance from the voltage source, whereas the bus 10 is connected to all branches of the RDN. Therefore, these three buses (10,22,30) are the candidate buses for optimum location of SSG units. Bus 2 represents the slack bus.

Figure (4.4) and (4.5) illustrate the P-V curves for candidate buses and loading parameter λ_{\max} value which determines the VSM.

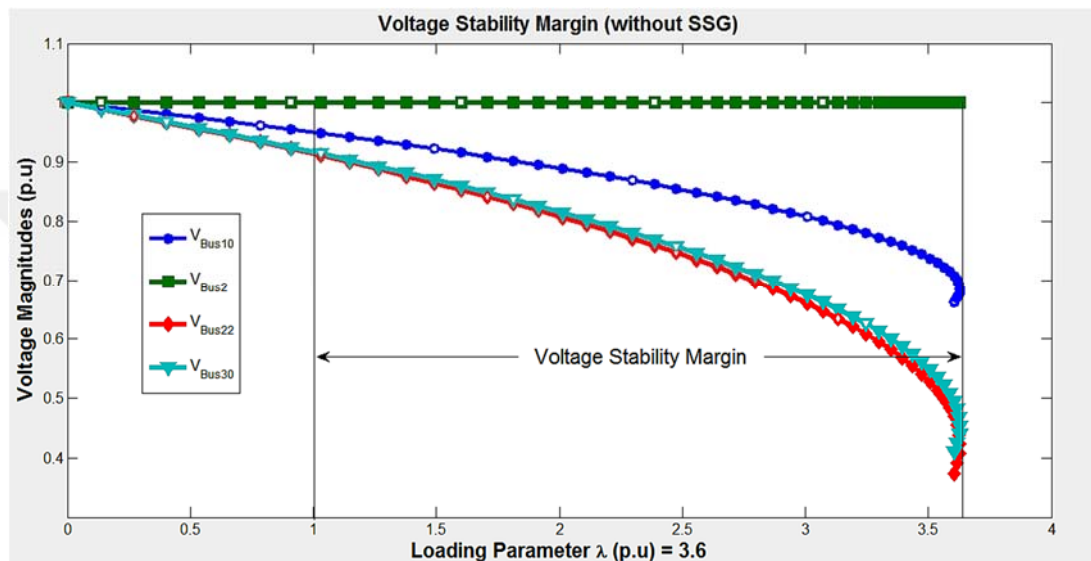


Figure 4.4: Voltage stability margin (without SSG).

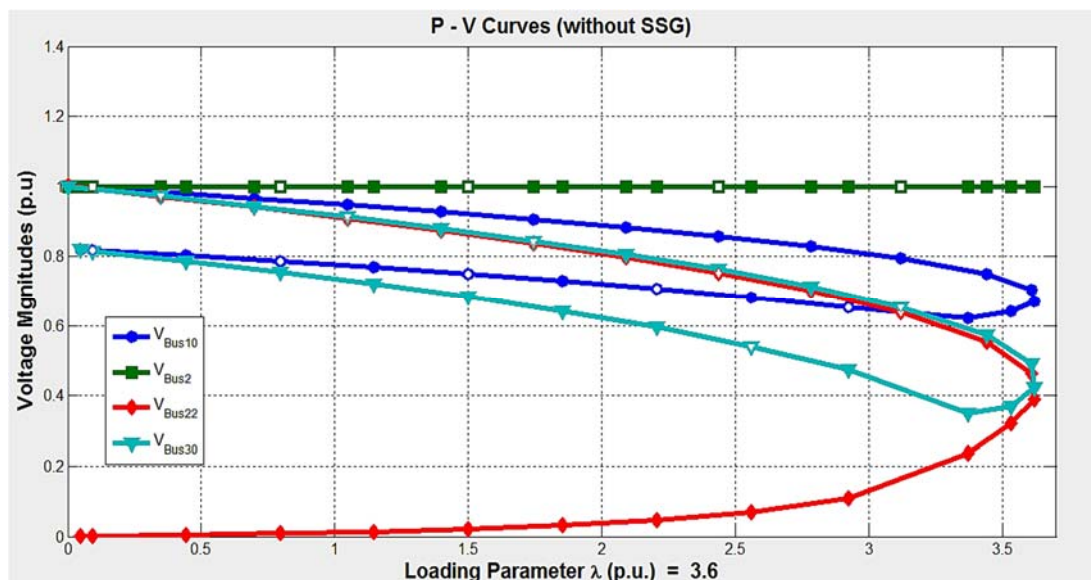


Figure 4.5: P-V Curves (without SSG).

Appendix (B.3) shows the loading parameters and voltages profile report for candidate buses. λ_{\max} is equal 3.6 p.u (without SSG).

4.4 Optimum Location and Capacity of SSG Units

Loss Sensitivity Factor technique was used to allocate the SSG units at optimum location among the candidate buses (10,22,30). Two stages were implemented to find optimum location and optimum capacity of SSG units as follows:

Stage One: Optimum location

1. Utilizing a PV Generator with capacity 50% of the total load and integrate it at each bus (10,22,30) individually.
2. Performing power flow analysis for each place of PV Generator in the candidate buses (10,22,30) separately in order to determine the total active power losses at each location of the proposed SSG unit.
3. Calculating LSF for each different location of SSG unit. The negative value of LSF represents the optimum location of SSG unit. (review equation 3.24).

Table (4.3) shows the results of stage one. The SSG unit which is used for the test is a PV Generator with rated 12.66 kV and 1.85 MW (50% of total load of the network).

Table 4.3: Results of optimum SSG location.

Case	Total power losses MW	LSF		
		SG size 30%	SG size 50%	SG size 80%
Without DG	0.196	X	X	X
DG at bus 10	0.056	- 0.122	- 0.074	- 0.043
DG at bus 22	0.892	+ 0.282	+ 0.374	+ 0.405
DG at bus 30	0.345	+ 0.073	+ 0.08	+ 0.104

$$LSF_{(SSG \text{ at bus } 10)} = \frac{(0.056 - 0.196)MW}{1.85 MW} = - 0.074$$

It is obvious from the results that the integration of the SSG unit at **bus10** had reduced the total active network power losses. Moreover, the LSF has a negative value which means that **bus10** is the optimum location for the SSG unit among other candidate buses.

Figure (4.6) illustrates the total power losses of the network when SSG unit was integrated with incremental capacities at different buses (10,22,30). It shows that when SSG unit is integrated at **bus10** the network has minimum total power losses.

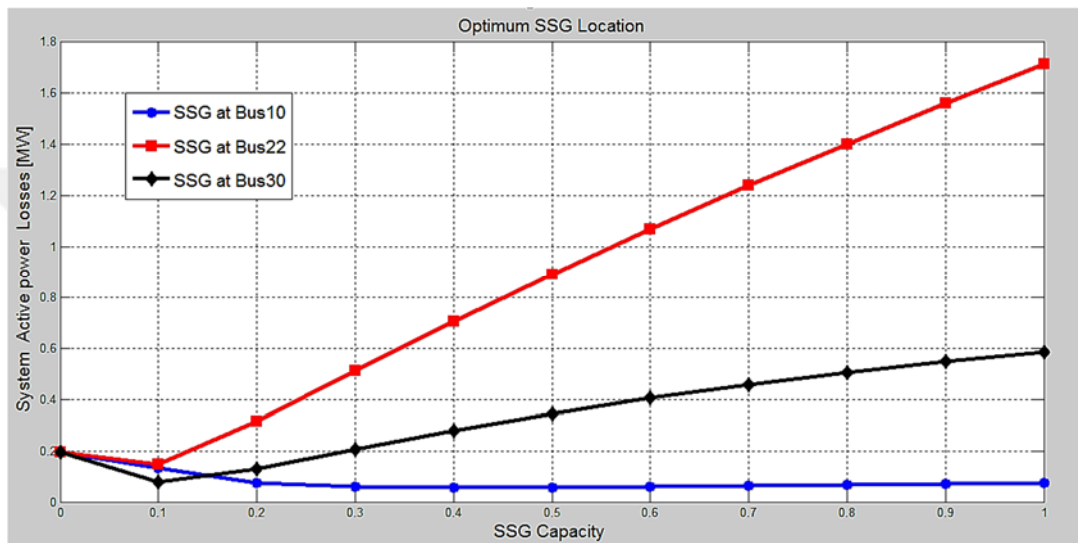


Figure 4.6: Network total power losses with SSG at different busses.

Stage Two: Optimum Capacity

The optimum capacity can be obtained as follows:

1. Penetrating SSG unit at bus10 with incremental capacities starts with 10% to 100% of the total load of the network.
2. Performing the power flow analysis for each DG capacity.
3. The SSG unit capacity which gives the minimum total power losses represents the optimum SSG capacity.

Figure (4.7) depicts the optimum capacity of SSG unit. It is clear that the SSG capacity (1.5 MW) which is equal to 40% of total load (3.7 MW) is the optimum size that gives minimum power loss (0.056 MW).

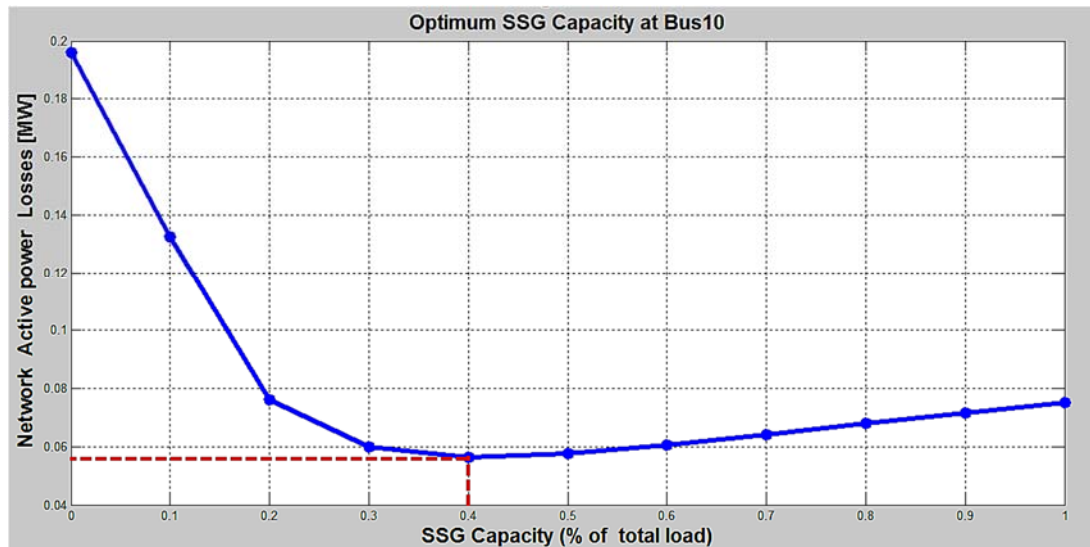


Figure 4.7: Optimum SSG unit capacity.

All in all, (1.5 MW / 12.66 kV) for different types of SSG units which allocated at bus10 were used in voltage stability analysis.

Table (4.4) shows the impact of optimum capacity of SSG unit on central power generation of the central utility which is consumed by the network loads and its influence on active and reactive power losses in the DN.

Table 4.4: The impact of optimum capacity of SSG unit on utility power and DN losses.

Case	Central power generation MW	Active power losses MW	Reactive power losses MVAR
Without SSG	3.9	0.196	0.105
SSG at bus10	1.3	0.056	0.016
SSG at bus22	1.5	0.705	0.543
SSG at bus30	1.4	0.278	0.197

4.5 Voltage Stability Static Analysis Results

CPF technique was used in the static analysis.

4.5.1 Photovoltaic SSG Unit (PVG)

4.5.1.1 Voltage Control Operation Mode

(PV Generator Model) SSG unit with rated voltage 12.66 kV and rated power 1.5 MW was connected at bus10. Figures (4.8) shows the integration impact of PV generator on loading parameter using GUI.

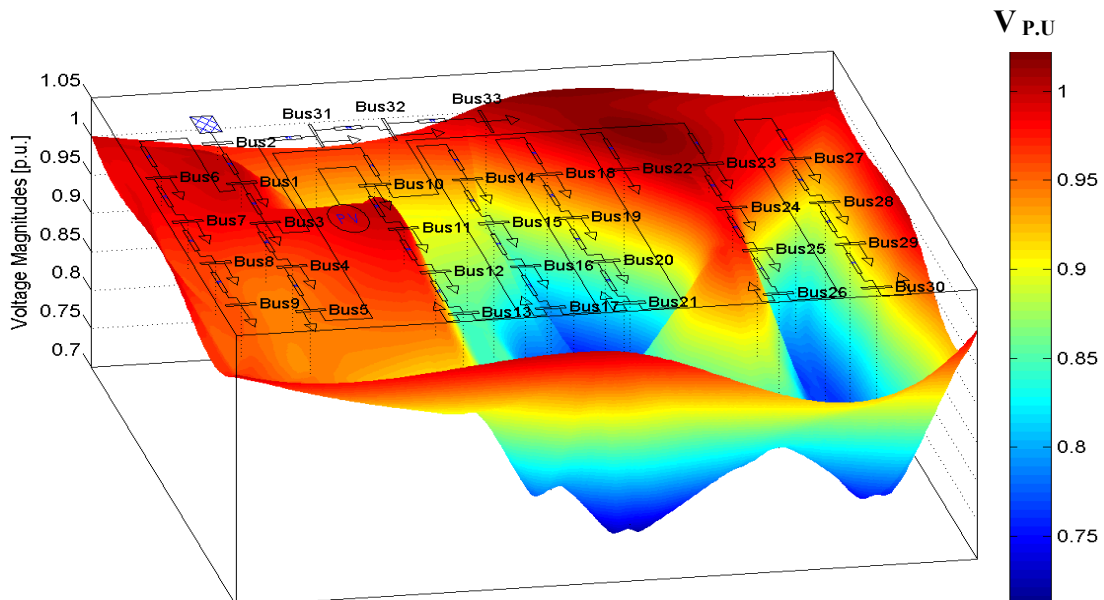
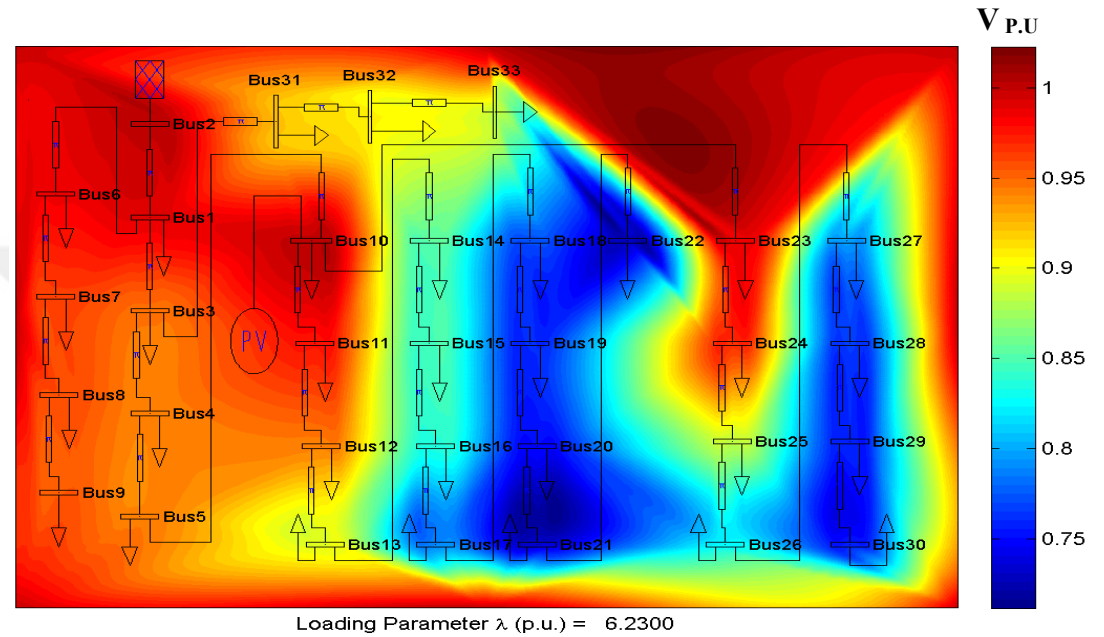


Figure 4.8: Integration Impact of a PV Generator using GUI.

Figure (4.9) illustrates λ -V curves for buses (2,10,22,30) when a PV generator was integrated into DN. It is clear that the voltage stability margin was improved and loading parameter λ_{max} was increased from 3.6 p.u (without DG) to 6.23 p.u . The voltages profile of the buses was improved too.

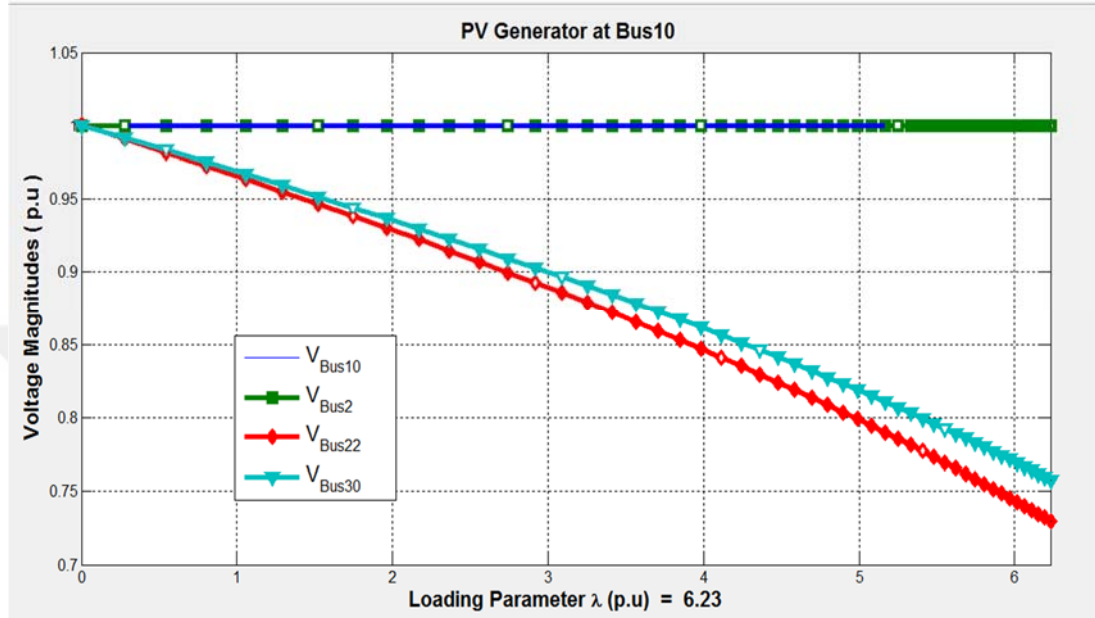


Figure 4.9: λ -V Curves when a PV generator was integrated into DN.

4.5.1.2 Power factor control operation mode

(PQ Generator Model). This DG model produces both active and reactive powers and maintain the power factor value constant during operation.

Let's suppose that the SSG unit has $\cos \theta = 0.85 \text{ lag}$, 1.5 MW and by applying the equation (3.6) the reactive power can be calculated. It is equal to 0.92 MVAR.

This model slightly enhances the VSM and does not affect on buses voltages profile but reduces the power losses in DN.

4.5.2 Reactive Power Control Operation Mode

(Q Generator Model). In this model the reactive power is produced as a function of bus voltage, therefore the buses voltages profile have high values compared with other models, but VSM ,in this case, is less than which in PV and PQ

generators models due to the absence of active power production in this proposed model ($P = 0$).

Table (4.5) depicts the static analysis results of DN integrated with Photovoltaic generator in different operation modes.

Table 4.5: Static analysis results of the DN with static SSG models.

SSG Type	Network (P) Losses MW	Network (Q) Losses MVAR	λ_{max} p.u	(V) bus 22 p.u	(V) bus 30 p.u
Base Case	0.20	0.11	3.6	0.46	0.49
PV Gen.	0.06	0.02	6.2	0.72	0.75
PQ Gen.	0.08	0.03	3.9	0.42	0.46
Q Gen.	0.37	0.22	3.7	0.85	0.87

The results above show that the PV generator (voltage control operation mode) is the best model among others to develop the voltage stability margin due to high Loading parameter value. Also, the buses voltages profile is improved.

The PQ generator model is used to reduce the total power losses in the network. However, the buses voltage stability was slightly improved, Whereas the Q generator model improved the buses voltages profile.

4.5.3 Solid Oxide Fuel Cell SSG

The parameters of the FC-SSG were illustrated in Appendix (C.1). Figure (4.10a) and (4.10b) shows the model and its λ -V curves respectively.

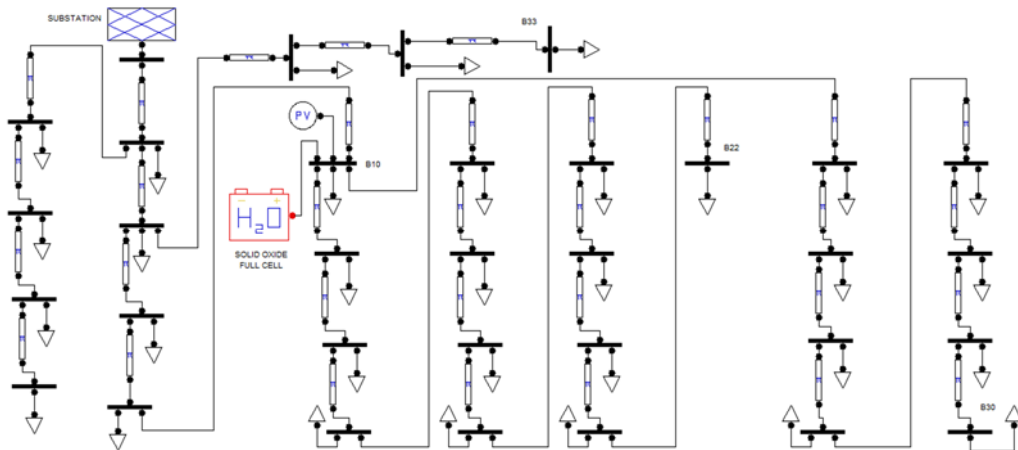


Figure 4.10a: DN integrated with FC-SSG model.

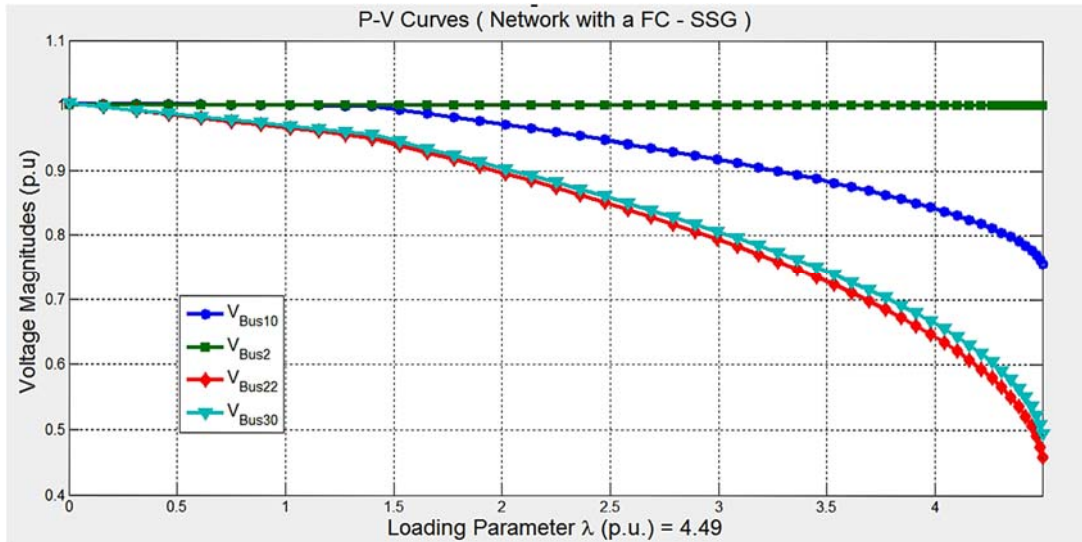


Figure 4.10b: λ -V curves (Network with a FC-SSG).

4.5.4 Constant Speed Wind Turbine with Induction generator Model

Squirrel Cage Induction generator model was connected to the DN. The induction generator model parameters and wind model were illustrated in Appendix (C.2) and (C.3) respectively. Figure (4.11a) shows the radial DN integrated with SCIG wind turbine unit.

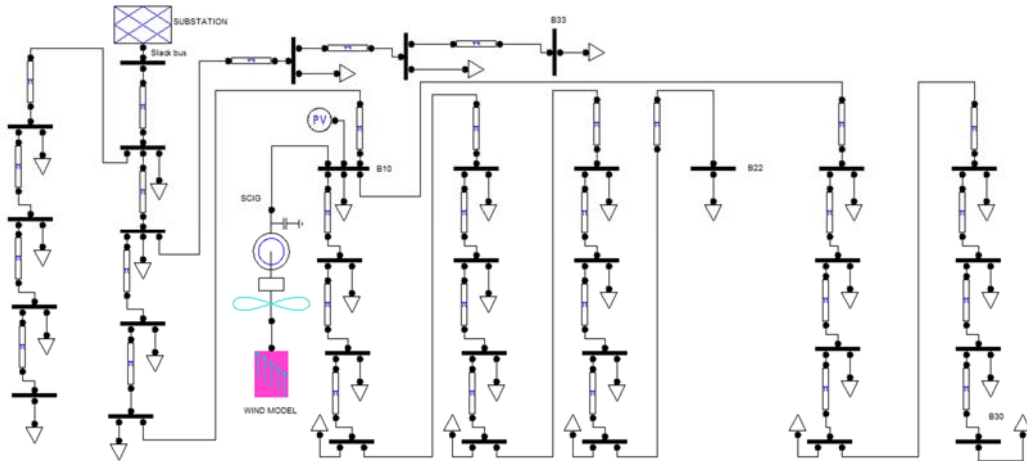


Figure 4.11a: DN integrated with SCIG unit.

The SCIG unit is connected with wind model which is available in PSAT models. λ -V curves which determine the VSM of the model are illustrated in Figure (4.11b).

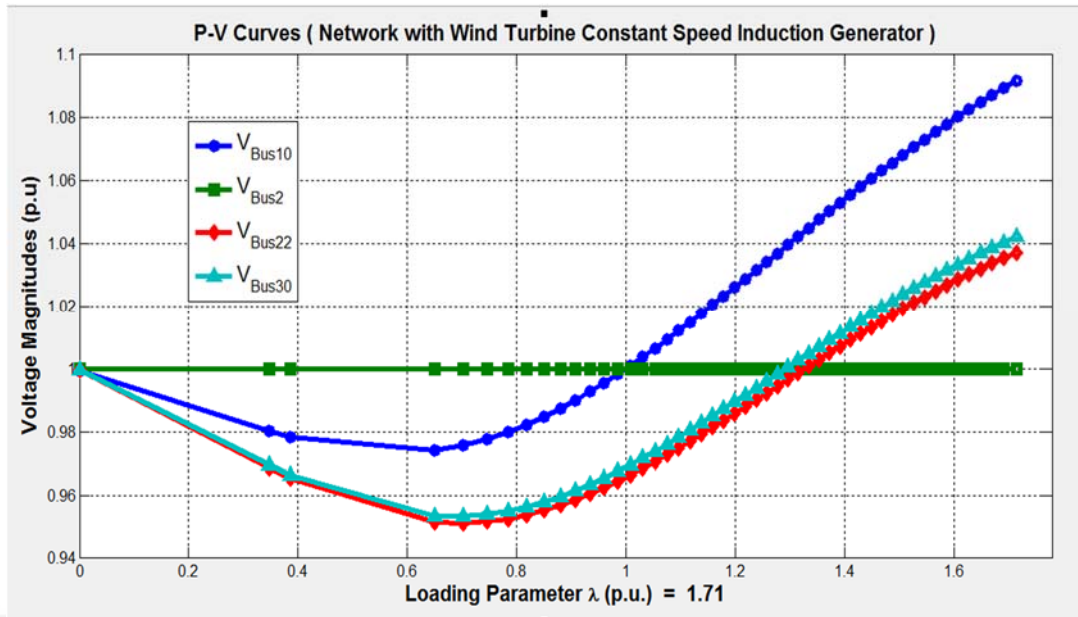


Figure 4.11b: λ -V curves for the network buses with CSWTIG unit.

4.5.5 Synchronous Generator Model

A synchronous generator was connected at DN has parameters which depicted in Appendix (C.4). Static analysis was applied using CPF technique illustrated in Figure (4.12).

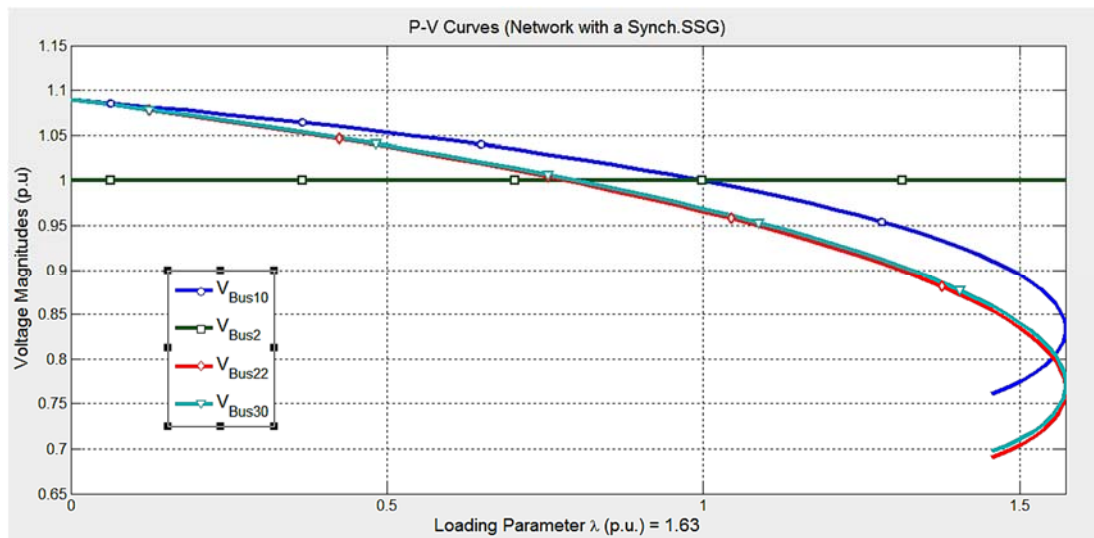


Figure 4.12: λ -V curves (Network with a Synch – SSG).

Table (4.6) shows the buses voltages profile and loading parameter values which represent the VSM for different SSG units models.

Table 4.6: Loading parameters of the DN with different SSG unit types.

Case	λ_{max} p.u	(V) bus 22 p.u	(V) bus 30 p.u
Without SSG	3.6	0.46	0.49
FC-SSG	4.5	0.45	0.49
WTIG	1.7	1.03	1.04
Synch. SSG	1.6	0.93	0.93

4.5.6 Discussion of the Static Analysis Results

The VS static analysis results examined the maximum loading parameters λ_{max} of different types of SSG units and showed that the static SSG units which based on power electronics converters such as photovoltaic and Fuel cell generators are effective for enhancing the VSM of the radial DN.

Furthermore, the optimum enhancement of the VS occurs when these static SSG units operate in voltage control operation mode (PV model). On the other hand, Dynamic units which are directly connected to the network such as Induction and Synchronous generators have a negative impact on VS of the network.

4.6 Voltage Stability Dynamic Analysis Results

The dynamic analysis was implemented using the time domain simulation. The aim of this analysis is to examine the steady state condition of the voltages magnitudes of DN buses when they were subjected to a disturbance.

In this work, an **Earth Fault** was applied at bus22, which has the weakest voltage magnitude, in order to simulate a virtual disturbance. Three different SSG units were utilized individually and connected at bus10 in this proposed analysis; FC unit, Synch. unit, and CSWTIG unit. The fault duration time was set to (0.1) second and plotting time step Δt was set to (0.05) second.

4.6.1 Network Dynamic Analysis without SSG unit

Figure (4.13) shows an earth fault model applied on bus22

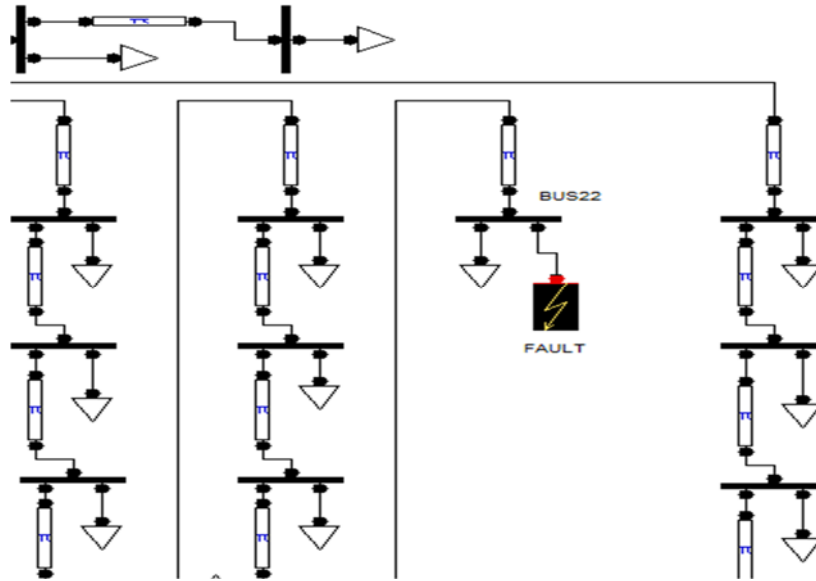


Figure 4.13: Earth fault model.

Figure (4.14) illustrates buses voltages magnitude when 0.1- second earth fault applied at bus22.

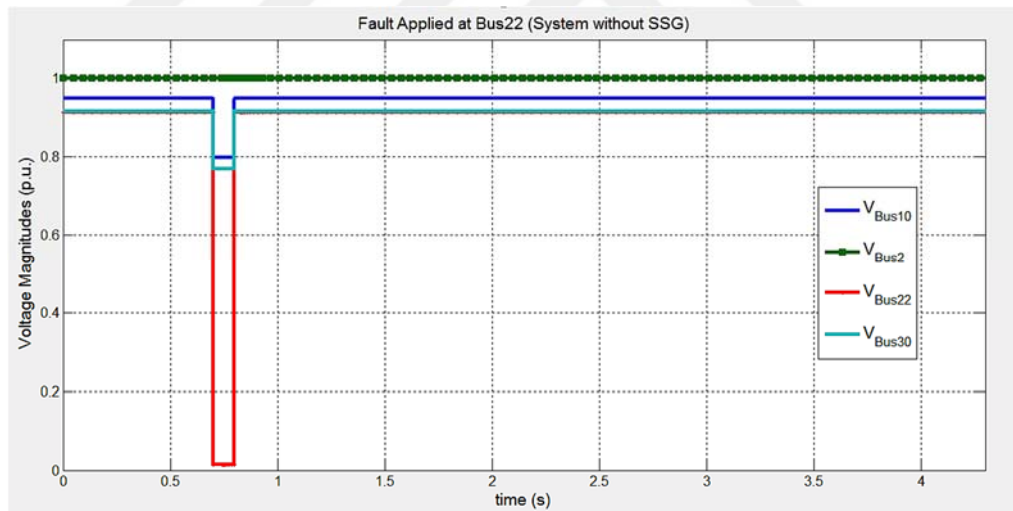


Figure 4.14: Time domain simulation of the network without SSG.

As shown from the figure above, buses voltages went back to its normal values after fault time was ended.

4.6.2 Network Dynamic Analysis with a FC-SSG Unit

Voltage magnitude of bus10, where FC-SSG was connected, is shown in Figure (4.15). The fault was applied at bus22.

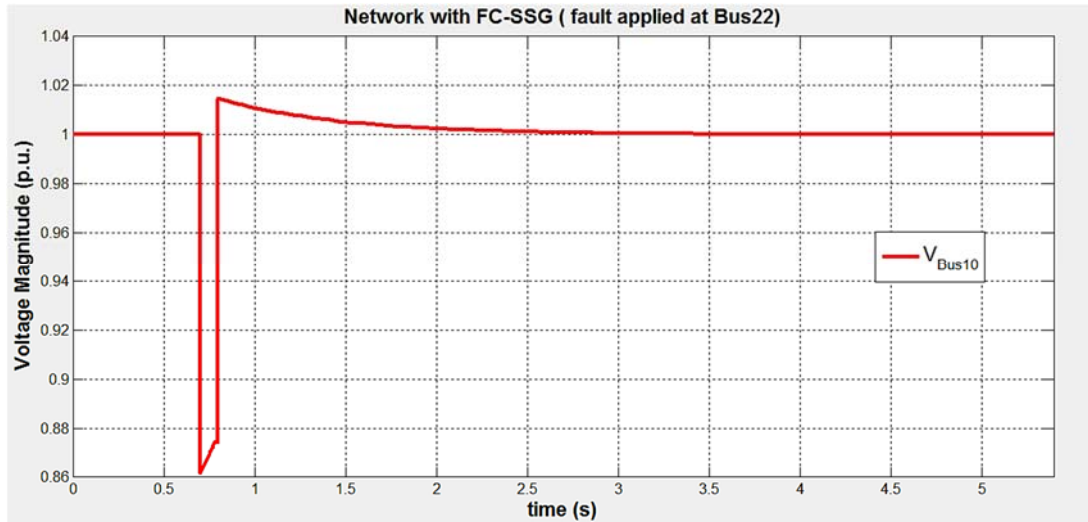


Figure 4.15: Time domain simulation of the network with a FC-SSG.

The bus10 voltage magnitude reached to the steady state condition after 1.8 second from the ending of fault time when FC-SSG was integrated into DN.

4.6.3 Network Dynamic Analysis With a Synch. Gen unit

Two scenarios were performed in this work; the first one was the integration of a synch. SSG without contribution of Automatic Voltage Regulator AVR. The simulation result is shown in Figure (4.16a). The second scenario was implemented using AVR model with the synch. Gen. Figure (4.16b) depicts the second scenario.

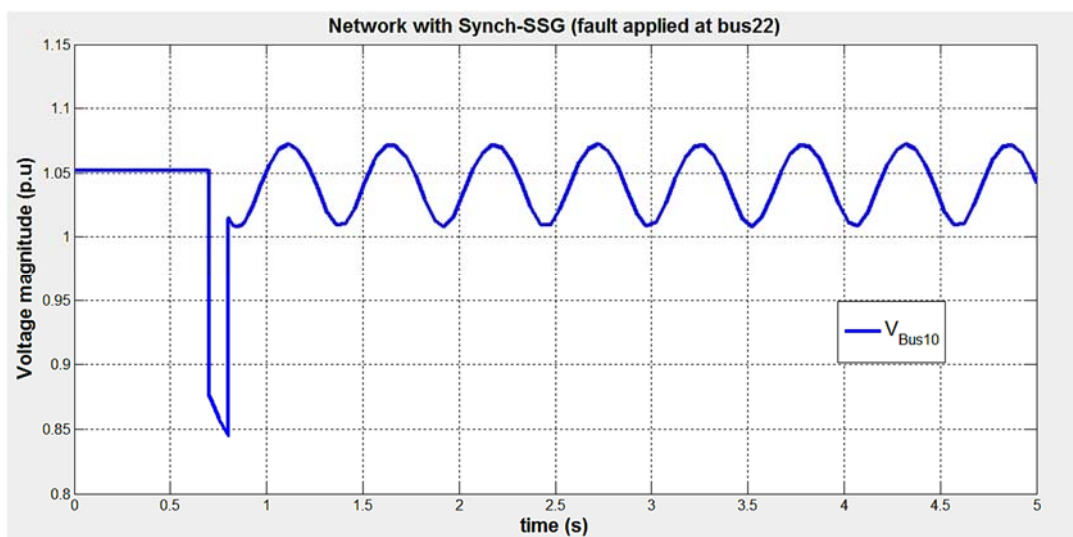


Figure 4.16a: Time domain simulation of the network with a Synch.SSG.

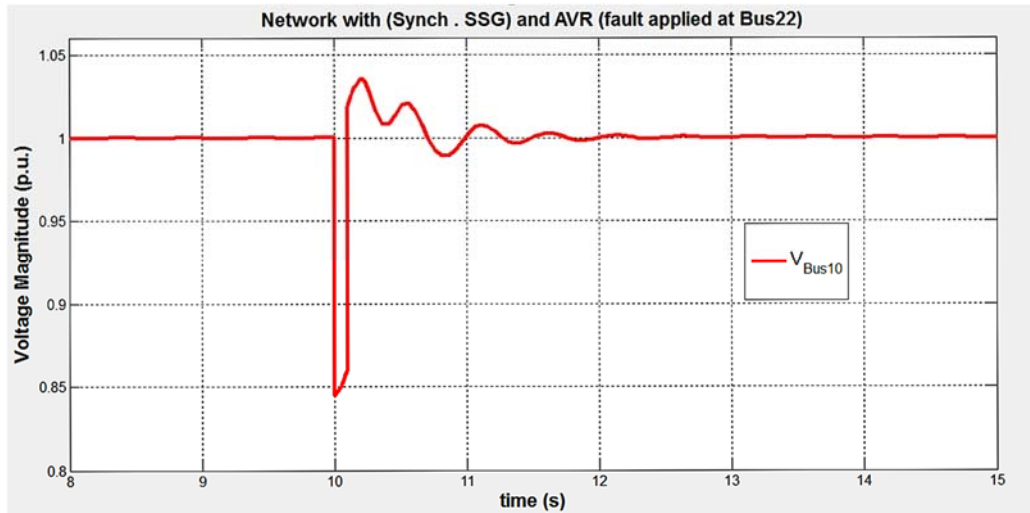


Figure 4.16b: Time domain simulation of the network with a Synch.SSG & AVR.

The voltage magnitude oscillates after disturbance with this type of SSG unit. An (AVR) (Appendix C.5) must always contribute in stabilization process. The steady state voltage was achieved in 4.1 seconds after fault time finish.

4.6.4 Network Dynamic Analysis With a CSWTIG Unit

Constant speed wind turbine squirrel cage induction generator model was used. The time domain simulation of the model during normal operation condition (No fault disturbance) showed that the bus voltages are flicker due to wind turbine mechanical control and turbulence. Figure (4.17) illustrates the voltage flicker of the wind turbine at bus10.

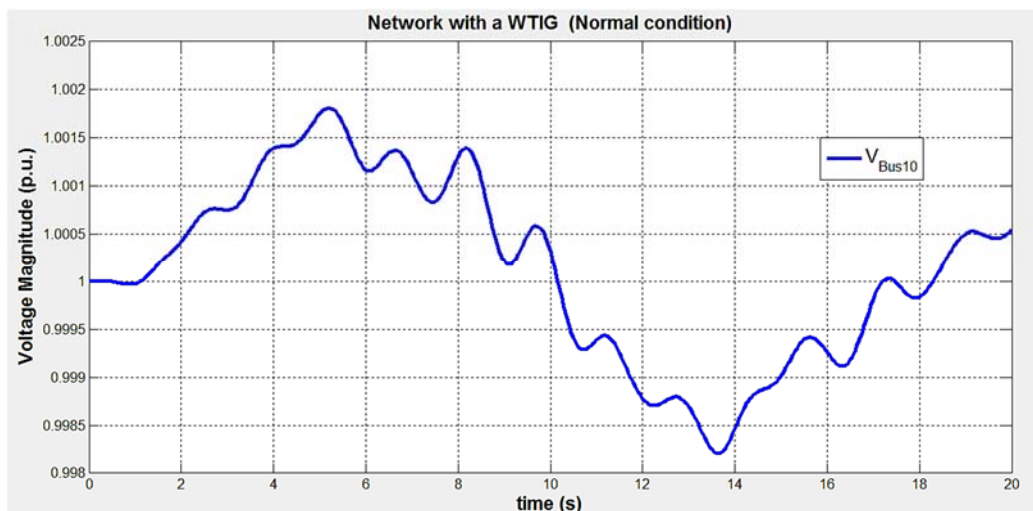


Figure 4.17: Voltage flicker of a CSWTIG at bus10.

The same fault scenario was applied on this model (0.1 S fault duration time at bus22 and the SSG unit was integrated at bus10). The buses voltages, in this case, are shown in Figure (4.18).

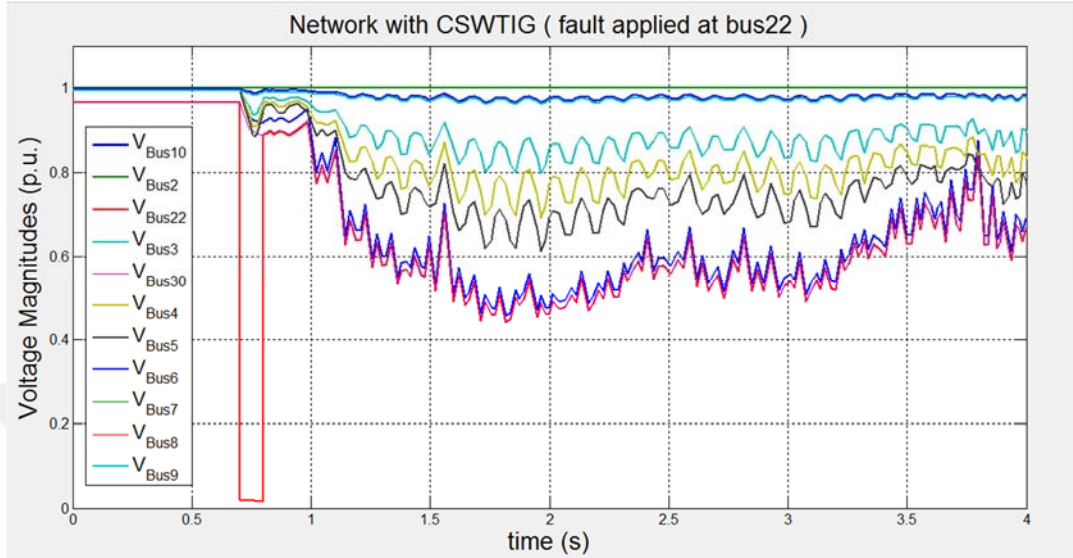


Figure 4.18: Time domain simulation of the network with a WTIG.

It is clear that the buses voltages are unstable after the fault occurrence because the squirrel cage induction generator absorbs a large amount of reactive power from DN during disturbances. This situation leads to voltage instability.

A solution was suggested in order to keep the system voltage in stable condition:

Disconnecting the WTIG unit from the DN in the case of the fault disturbance to prevent the induction generator from absorbing reactive power from the network. In order to avoid adding additional bus and disconnecting bus10 which feeds many buses with power, WTIG unit in this case connected to bus 22 and a Circuit Breaker was used to disconnect the WTIG from the network instantaneously in a fault condition. Figure (4.19) illustrates the network model.

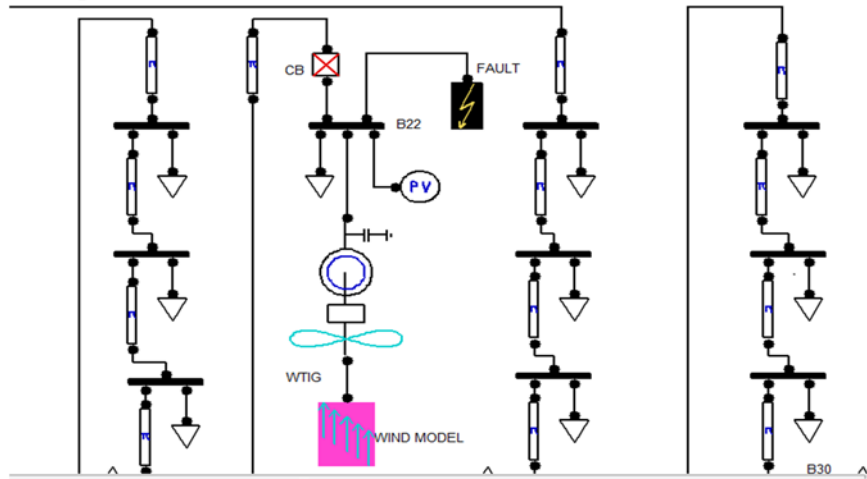


Figure 4.19: WTIG with fault and C.B models.

The CB time setting should be corresponding to the fault time setting in order to disconnect the WTIG in the same time with fault occurrence. Figure (4.20) shows voltage magnitudes after disconnecting WTIG from the network at $t = 0.7$ S.

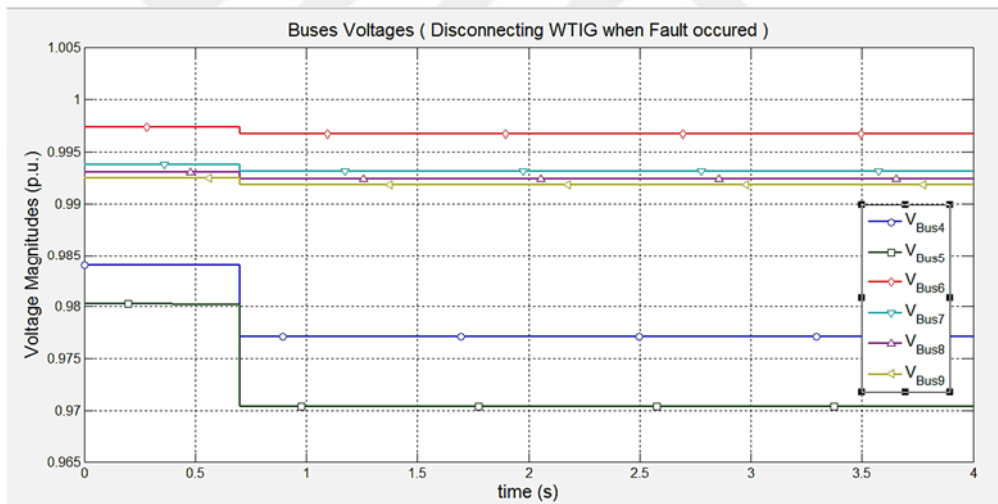


Figure 4.20: Time domain simulation (Disconnecting WTIG).

This method is useful to preserve the buses voltages in stable condition. The result shows that voltage value has a barely noticeable change when WTIG unit was disconnected.

4.6.5 Discussion of the Dynamic Analysis Results

The dynamic analysis results showed that the integrating of SSG units in DN increased the possibility of voltage instability during disturbances and contingencies

conditions. The results ensured that the static SSG units (which based on power electronic converters) have the least negative impact on VS among other SSG units types due to their fast damping response during turbulence. However, the synchronous generator unit must be attached with an AVR for oscillatory voltage damping which is formed during disturbance because of the dynamic order of the rotary machine. On the other hand, the constant speed WTIG unit has a negative influence on VS of network buses due to its consumption of reactive power during operation and high reactive power absorption in fault case.

Table 4.7: dynamic analysis results report for different SSG types.

SSG Type	V bus10 (p.u.)	Steady State Voltage Time Delay (S)
FC-SSG	0.86	1.8
Synch.SSG	0.85	4.1
WTIG	Unstable	Disconnecting WTIG Time

4.7 Small Signal Stability Analysis SSSA Results

Figures (4.21 a,b,c) depict the Eigenvalues for FC, Synch. DG, and WTIG units respectively in S-domain when they integrated into RDN.

4.7.1 Network With a FC-SSG Unit

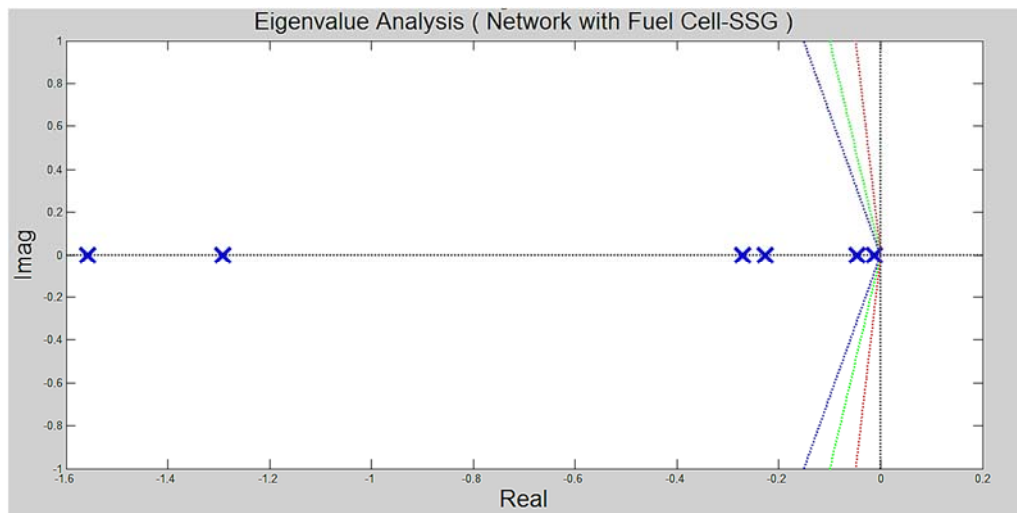


Figure 4.21a: Eigenvalues of the FC-SSG in the S-domain axis.

Table (4.8) shows the Eigenvalues analysis result of the FC-SSG integrated into DN.

Table 4.8: Eigenvalues of the FC-SSG.

Eig. No.	Real part	Imag. part
1	- 1.56	0
2	- 1000.00	0
3	- 1.29	0
4	- 0.27	0
5	-0.23	0
6	-0.05	0
7	-0.01	0

All the poles of the system are negative and they are on the left side of the S-domain, which means that the system buses voltages are stable during operation. And the system has no complex pairs. The Eigenvalue analysis report of the model exists in (Appendix D.1).

4.7.2 Network With a Synch. Gen Unit

Figure (4.22b) and Table (4.9) depict the Eigenvalue analysis of the Synch-Gen unit. (Appendix D.2) shows the Eigenvalue report of the model. This system is stable because all the real parts of poles and complex pairs exist in the negative half of the S-domain axis.

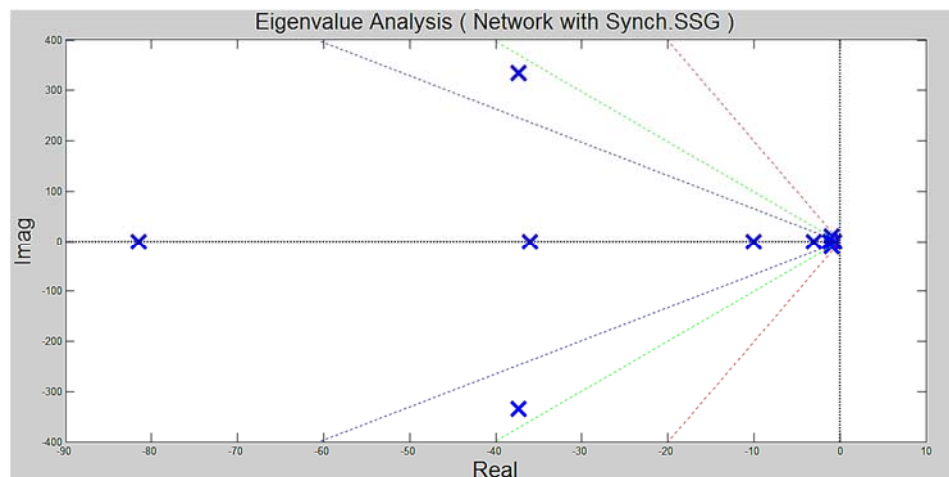


Figure 4.21b: Eigenvalues of the Synch.SSG in the S-domain.

Table 4.9: Eigenvalues of the Synch.SSG.

Eig. No.	Real part	Imag. part
1	-1	0
2	-10	0
3	-1000	0
4	-37.27	334.41
5	-37.27	-334.41
6	-81.43	0
7	-35.10	0
8	-0.89	10.32
9	-0.89	-10.32
10	-2.95	0
11	-0.66	0
12	-1.15	0

4.7.3 Network With a WTIG Unit

Figure (4.22c) shows the Eigenvalue analysis of the constant speed wind turbine squirrel cage induction generator. The analysis result is shown in the Table (4.9). (Appendix D.3) shows the analysis report.

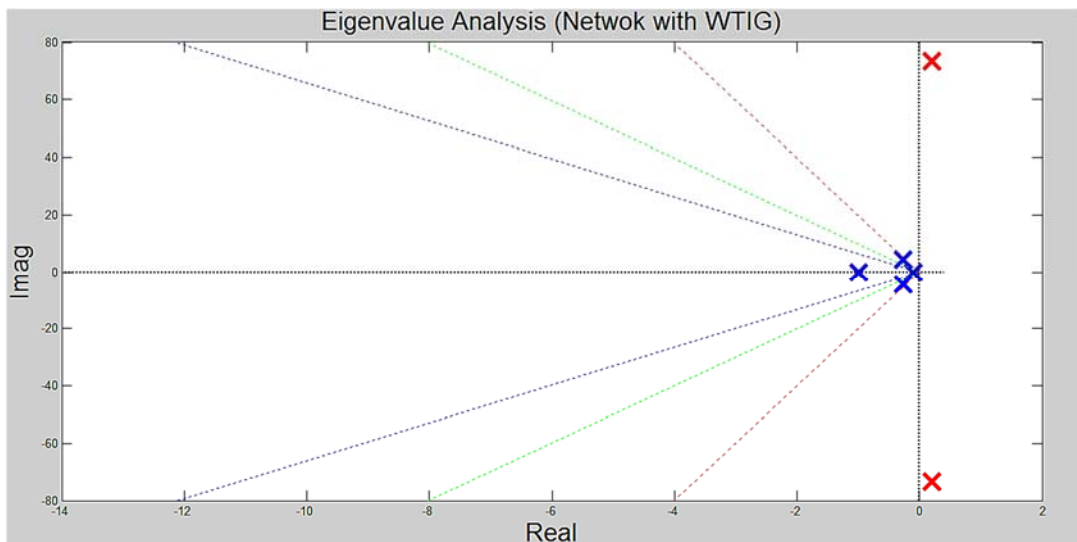


Figure 4.21c: Eigenvalues of the WTIG in the S-domain.

Table 4.10: Eigenvalues of the WTIG.

Eig. No.	Real part	Imag. part
1	0.21	73.50
2	0.21	- 73.50
3	- 0.99	0
4	- 0.26	4.30
5	- 0.26	- 4.30
6	-0.10	0

There are two poles on the right side of the S-domain axis, therefore the system voltage is not stable in case of constant speed wind turbine squirrel cage induction generator.

A solution was suggested to bring these two poles to the stable negative area of the S-domain axis. This solution was performed using a hybrid model by connecting a Synch. SSG at the same bus with the WTIG unit as shown in Figure (4.23).

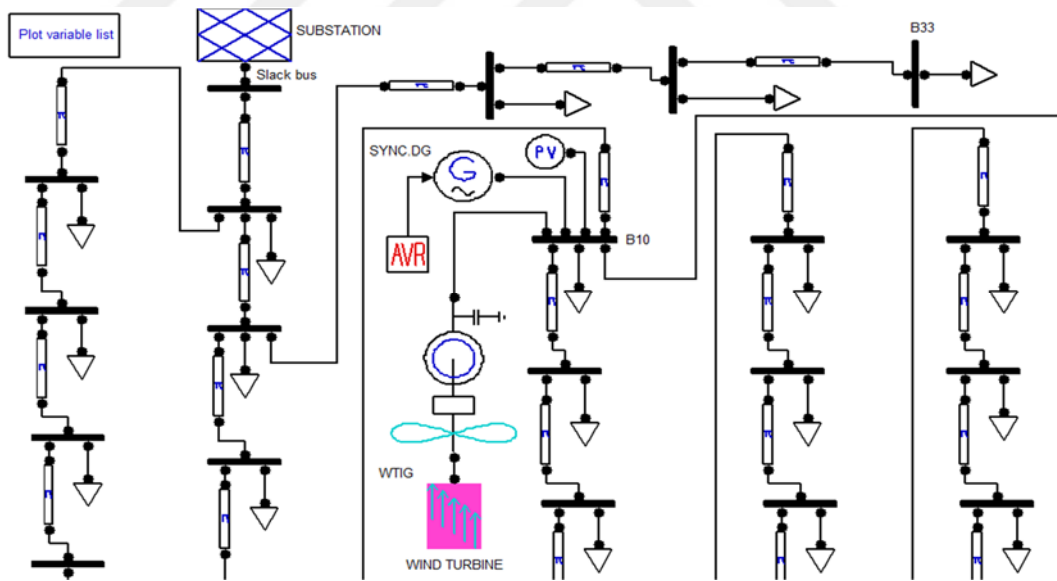


Figure 4.22: Hybrid model (WTIG unit & Synch-SSG).

Figure (4.24) shows the Eigenvalue analysis of the hybrid model. All the poles are exist in the left negative side of the S-domain axis. The model is considered a stable system.

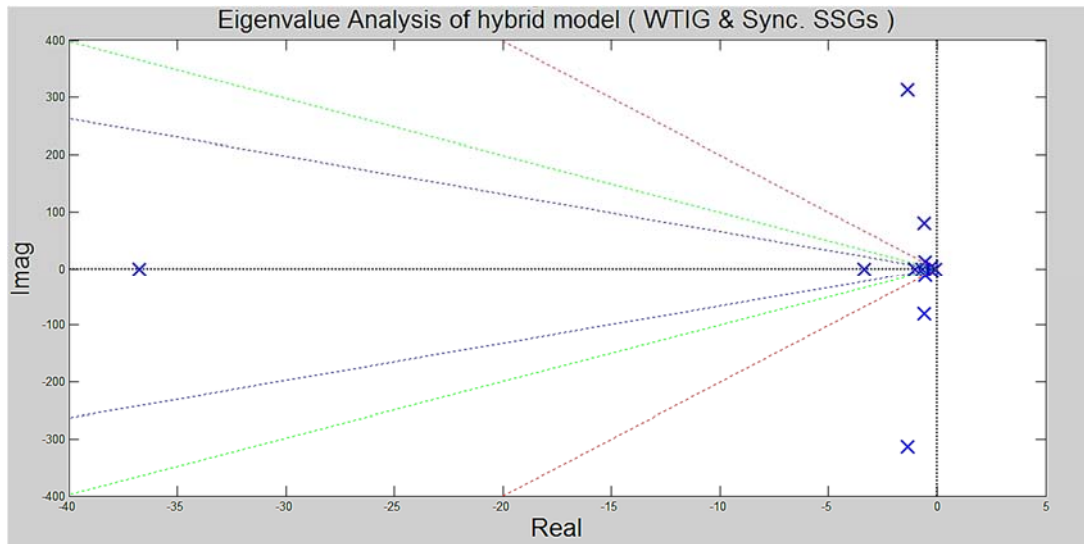


Figure 4.23: Eigenvalue of the hybrid model in the S-domain.

4.7.4 Discussion of the SSSA Results

SSSA analysis results were ensured and proved the dynamic analysis results which indicated that the radial distribution network voltages are not in stable condition with an individual and independent CSWTIG unit.

CHAPTER FIVE

CONCLUSIONS AND SUGGESTIONS FOR FUTURE WORK

5.1 Conclusions

This work presented the VS analysis of different types of SSG units integrated into a 33-bus radial distribution network. Different methods of VS analysis were used for each SSG type to investigate the VSM of the network in order to determine the most convenient SSG unit type that enhances the voltage stability of DN during normal operation and contingency condition using MATLAB/ PSAT Simulink. The obtained results proved that the static generators are better than the dynamic generator to improve the voltage stability margins and loadability of radial distribution network buses. On the other hand, constant speed wind turbine type squirrel cage Induction generator has a negative effect on and loadability whereas the synchronous generator has a batter impact on oscillatory stability during disturbance condition compared with squirrel cage constant speed wind turbine.

The main remarks can be summarized as follows:

1. In radial distribution network, the buses voltages magnitudes decrease whenever their locations are distant from the voltage source because of line losses and buses loads.
2. The Continuation Power Flow analysis CPF, which is available in PSAT, is useful to find the bus which has the weakest voltage magnitude among other buses. The network parameters visualization is available using Graphic User Interface GUI.
3. In radial distribution network, it is recommended to allocate the SSG units at the downstream bus which feeds a maximum number of branches with power. On the other hand, connecting SSG units at the last buses increases the total power losses of the network because the generated current from the SSG unit will flow in opposite direction and contracts the original current flow direction of the DN.

4. High - level capacity penetration of SSG units into radial distribution network increases the total power losses due to surplus injected power into the network. This additional power is dissipated in form of losses in the network lines.

5. Optimum location and capacity of SSG units which integrated in DN are crucial to decrease the total power losses and to reduce the drawn power amount from substation by DN loads.

6. According to static analysis of voltage stability, a static SSG unit type with electronic power converter such as (Photovoltaic or Fuel Cell) generator has the best effect on voltage stability margin and the network buses loadability, whereas the constant speed wind turbine with squirrel cage induction generator has the worst effect on voltage stability of DN. The squirrel cage induction generators consume reactive power from the network in order to generate active power, this condition will affect on voltage stability of the network.

7. The results showed that control operation modes of a static SSG unit type have different influences on DN as follows;

- a) Voltage control operation mode increased voltage stability margin and buses loadability with minimum lines losses.
- b) Power factor control operation mode has a small positive impact on voltage stability and no improvement in buses voltages magnitudes were observed.
- c) Reactive power control operation mode had enhanced buses voltages profile with some improvement in voltage stability.

8. The dynamic analysis was implemented using time domain simulation which showed that the DN voltage stability had affected negatively during disturbance when it was integrated with SSG units. In other words;

- a) FC unit, which is based on power electronic converter, has a fast damping voltage response without oscillation after disturbance.
- b) Synch unit oscillates voltages magnitudes of the buses after the fault. Using an adequate AVR this oscillation will be suppressed in 4.1 seconds.
- c) WTIG unit has negative impact on voltage stability because of its consumption of reactive power from DN during normal operation condition and after disturbance. For this reason, the reactive power must be provided either from a main central power source or compensated from an external electronic device. It is recommended to disconnect CSWTIG from the

distribution network Instantaneously after excessive faults occurrence in order to preserve the buses voltages in stable condition.

9. Small signal stability analysis using frequency domain simulation proved that the FC and Synchron. SSG units have Eigenvalues in stable region of the S - domain axis, while WTIG has Eigenvalues in unstable area.

10. Using a hybrid model by connecting a Synchron. SSG unit at the same bus with the WTIG unit made all the poles exist in the negative (left) side of the S-domain axis. This model is considered a stable system.

11. Existence of harmonics is one of the voltage stability problems that produced in distribution networks because of the SSG units which are interfaced to the network through power electronic inverters. The network components and customer equipment are affected negatively when harmonics exceed a certain level.

5.2 Suggestions For Future Work

This work can be extended and developed by applying the proposed voltage analysis methods with different types of SSG units integration on a residential distribution network. Moreover, other types of SSG units such as a micro-turbine generator and a variable speed wind turbine with a synchronous generator can be examined according to their effect on voltage stability of the distribution network. Furthermore, studying the effect of harmonics on voltage stability, can be thoroughly investigated.

REFERENCES

- [1] P. Kundur, N. J. Balu, and M. G. Lauby, *Power System Stability and Control*: McGraw- Hill Professional, 1994.
- [2] N. Hadjsaid, J. F. Canard, and F. Dumas, "Dispersed generation impact on distribution networks," *IEEE Comput. Appl. Power*, vol. 12, pp. 22- 28, 1999.
- [3] P. Kundur, J. Paserba, V. Ajjarapu, G. Andersson, A. Bose, C. Canizares, N. Hatziargyriou, D. Hill, A. Stankovic, C. Taylor, T. Van Cutsem, And V. Vittal, "Definition and classification of power system stability IEEE/CIGRE joint task force on stability terms and definitions definitions, " *IEEE Trans. Power Syst.*, vol. 19, pp. 1387-1401, 2004.
- [4] R. S. A. Abri, E. F. El - Saadany, and Y. M. Atwa, "Distributed Generation placement and sizing method to improve the voltage stability margin in a distribution system," in *Proc. Electric Power and Energy Conversion Systems (EPECS)*. 2011.
- [5] R. S. A. Abri, "Voltage Stability Analysis with high Distributed Generation (DG) Penetration" *A thesis presented to the university of Waterloo, Ontario, Canada, 2012.*
- [6] P. Dondi, D. Bayoumi, C. Haederli, D. Julian, and M. Suter, "Network Integration of distributed power generation," *J. Power Sources*, vol.106, pp. 1-9, 2002.
- [7] R. C.Dugan and M. F. Mc Granaghan, *Electrical Power System Quality*, 2nd ed. New York: McGraw-Hill, 2002.
- [8] *IEEE Std 1547-2003*, "IEEE Standard for Interconnecting Distributed Resources with Electric Power Systems," 2003.
- [9] F. Blaabjerg, C. Zhe, and S. B. Kjaer, "Power electronics as efficient Interface in Dispersed power generation systems," *IEEE Trans. Power Electron.*, vol. 19, pp. 1184-1194, 2004.
- [10] T. Ackermann, *Wind Power in Power Systems*: John Wiley & Sons, 2005.

- [11] M. Uzunoglu, O. Onar, M. Y. El-Sharkh, N. S. Sisworahardjo, A. Rahman, and M.S. Alam, "Parallel operation characteristics of PEM fuel cell and micro turbine power plants," *J. Power Sources*, vol. 168, pp. 469-476, 2007.
- [12] L. Li-Shiang, H. Wen-Chieh, F. Ya-Tsung, and C. Yu-An, "Novel grid-connected photovoltaic generation system," in *Electric Utility Deregulation and Restructuring and Power Technologies (DRPT)* pp. 2536-254, 2008.
- [13] R. S. Alabri and E. F. El-Saadany, "Interfacing control of inverter based DG units," in *Proc. International Conference on Communication, Computer and Power (ICCCP'09)*. SQU, Oman, 2009.
- [14] Rajendra Prasad Payasi, Asheesh K. Singh, Devender Singh, "Planning of different types of distributed generation with seasonal mixed" load models, 2012.
- [15] T. Ackermann, G. Andersson, and L. Sdger, "Distributed generation: a definition," *Electr. Power Syst. Res.*, vol. 57, pp. 195-204, 2001.
- [16] H. Zareipour, K. Bhattacharya, and C. A. Cañizares, " Distributed Generation: Current Status and Challenges" NAPS, Power and Energy Systems Group, Department of Electrical and Computer Engineering, University of Waterloo, Canada.
- [17] Stefan C.W. Krauter, *Solar Electric Power Generation – Photovoltaic Energy Systems*:Rio de Janeiro RJ Brazil, 2006.
- [18] Mukund R. Patel, *Wind and Solar Power Systems -Design, Analysis, and Operation*: U.S. Merchant Marine Academy Kings Point, New York, U.S.A.
- [19] Behnam Tamimi, Claudio Cañizares, and Kankar Bhattacharya, "Modeling and Performance Analysis of Large Solar Photo-Voltaic Generation on Voltage Stability and Inter-area Oscillations" IEEE *Trans.* Department of Electrical and Computer Engineering at the University of Waterloo, Waterloo, Canada, 2011.
- [20] Marcelo Gradella Villalva, Jonas Rafael Gazoli, and Ernesto Ruppert Filho Comprehensive Approach to Modeling and Simulation of Photovoltaic Arrays Arrays IEEE *Trans. Power Electronics*, Vol. 24, No 5, May 2009.
- [21] Gonggui Chen, Jinfu Chen, and Xianzhong Duan, "Power Flow and Dynamic Optimal Power Flow Including Wind Farms," National Basic Research Program of China (973 Program) (2009CB219700) and the Science Research Program of Education, Bureau, China.

- [22] D. M. Ali, "A simplified dynamic simulation model (prototype) for a stand-alone Polymer Electrolyte Membrane (PEM) fuel cell stack," in Proc. *International Middle-East, Power System Conference, MEPCON*, pp. 480-485, 2008.
- [23] A. M. Azmi, "Simulation and Management of Distributed Generating Units using Intelligent Techniques" vol. Ph.D. dissertation, University of Duisburg - Essen, Germany, 2005.
- [24] M. W. Ellis, M. R. Von Spakovsky and D. J. Nelson, "Fuel cell systems: efficient, flexible energy conversion for the 21st century" Proceedings of the IEEE, Vol. 89, Issue: 12, Dec. 2001, pp. 1808-1818.
- [25] K. Y. Ho and K. S. Sun, "An electrical modelling and fuzzy logic control of a fuel cell generation system" *Energy Conversion, IEEE Transactions on*, Vol. 14, No. 2, June 1999.
- [26] W. Shepherd, L. N. Hulley and D. T. W. Liang, "Power electronics and motor control" 2nd edition, Cambridge University Press, New York, NY, USA, 1995.
- [27] C. Sharma, "Modeling of an Island Grid" *Power Systems, IEEE Transactions on*, Vol. 13, Issue. 3, August 1998, pp. 971-978.
- [28] W. G. Scott, "Micro - Turbine Generators for Distribution Systems," *IEEE Applications Magazine*, Vol. 4, Issue 4, pp. 57-62, May/June, 1998.
- [29] M. H. Rashid, "Power electronics - circuits, devices and applications" 2nd Edition, Prentice- Hall, New Jersey, 1993.
- [30] P. F. Ribeiro, B. K. Johnson, M. L. Crow, A. Arsoy, and Y. Liu, "Energy storage systems for advanced power applications," *Proceedings of the IEEE*, vol. 89, pp. 1744-1756, 2001.
- [31] Application Guide to the European Standard EN 50160 on "Voltage Characteristics of Electricity Supplied by Public Distribution Systems", *Electricity Product Characteristics and Electromagnetic Compatibility*, July, 1995.
- [32] Emanuel Widlund, "Power Quality Disturbances in Production Facilities," Department of Energy & Environment, University of Technology, Göteborg, Sweden, 2012.

- [33] Soens J, Driesen J and Belmans R., " Interaction between Electrical Grid Phenomena and the Wind Turbine's Behavior ", K. U. leuven, Department of Electrotechnical Engineering Esat - Electa, Heverlee, Belgium, 2004.
- [34] T. Ackermann and V. Knyazkin, "Interaction between distributed generation and the distribution network: operation aspect" IEEE/PES Transmission and Distribution Conf. and Exhibition 2002: Asia Pacific, Vol. 2, 6-10 Oct. 2002, pp. 1357-1362, Yokohama, Japan.
- [35] A. Agustoni, M. Brenna, R. Faranda, E. Tironi, C. Pincella and G. Simioli, "Constraints for the interconnection of distributed generation in radial distribution systems" Harmonics and Quality of Power, 10th International Conference on, Vol. 1, 6-9 Oct. 2002, pp. 310-315, Rio de Janeiro, Brazil.
- [36] J. H. R. Enslin, W. T. J. Hulshorst, A. M. S. Atmadji, P. J. M. Heskes, A. Kotsopoulos, J. F.G. Cobben, and P. Van der Sluijs, "Harmonic Interaction between Large numbers of photovoltaic inverters and the distribution network," in *Proc. IEEE Power Tech Conference, in Bologna*, Vol.3, p. 6, 2003.
- [37] F. Milano, "An open source power system analysis toolbox," IEEE Trans. Power Syst., Vol. 20, No. 3, pp. 1199-1206, Aug. 2005.
- [38] B. Venkatesh,, R. Ranjan, and H. B. Gooi, "Optimal reconfiguration of radial distribution systems to maximize loadability," *IEEE Trans. Power Syst.*, vol.19, pp. 260–266, 2004.
- [39] Shiqiong Tong, and Karen Nan Miu, "A Network-Based Distributed Slack Bus Model for DGs in Unbalanced Power Flow Studies," *IEEE Trans. Power Syst.*, vol. 20, NO. 2, pp. 835 – 842, MAY 2005.
- [40] Y. Wenyu, Y. Xuying, D. Jiandong, W. Xiaozhong, F. Yue, "Power Flow Calculation Distribution Networks Containing Distributed Generation", Xi'an University of Technology, Xi'an Shanxi, China, 2008.
- [41] Federico Milano, Power System Analysis Toolbox Documentation for PSAT version 2.0.0, February 14, 2008.
- [42] C. Guo, X. Yan, Yang Wang, Y. Sun, C. Yuan, Q. Jiang, "Research On Power Load Flow Calculation for Photovoltaic-ship Power System based on PSAT", 4th International Conference on Renewable Energy Research and Applications, Palermo Palermo, Italy, 22-25 Nov 2015.

- [43] V. Knyazkin, L. Soder, C. Canizares, “Control Challenges of Fuel Cell – Driven Distributed Generation”, IEEE Bologna Power Tech Conference, June 23-26, Bologna, Italy, 2003.
- [44] W. F. Tinney and C. E. Hart, “Power Flow Solution by Newton’s Method,” IEEE Transactions on Power Apparatus and Systems, vol. PAS-86, pp. 1449–1460, Nov. 1967.
- [45] C. Hsiao-Dong and R. Jean-Jumeau, "Toward a practical performance Index for predicting voltage collapse in electric power systems," *IEEE Trans. Power Syst.*, vol. 10, pp. 584-592,1995.
- [46] C. A. Cañizares, *Voltage Stability Assessment: Concepts, Practices and Tools*, IEEE/FES Power System Stability Subcommittee Aug. 2002.
- [47] C. A. Canizares and F. L. Alvarado, "Point of collapse and continuation methods for large AC/DC systems," *IEEE Trans. Power Syst.*, vol. 8, pp. 1-8, 1993.
- [48] Mohamed M. Aly, Mamdouh Abdel-Akher, “A Continuation Power- Flow for Distribution Systems Voltage Stability Analysis”, IEEE International Conference of Power and Energy (PECon), Kota Kinabalu, Malaysia, 2-5 December 2012.
- [49] K. E. Brenan, S. L. Campbell, and L. Petzold, “Numerical Solution of Initial – Value Problems in Differential - Algebraic Equations”. Philadelphia, PA: SIAM, 1996.
- [50] D. Rakesh Chandra, M. S. Kumari, M. Sydulu, F. Grimaccia, M. Mussetta, S. Leva, M.Q. Duong.” Small Signal Stability of Power System with SCIG, DFIG Wind Turbines”. Annual IEEE India Conference (INDICON), 2014.
- [51] +EE4107 – Cybernetics Advanced, “Stability Analysis (Solutions)”, Faculty of Technology, Porsgrunn, Norway.
- [52] Zhaoyang Wei, Song Shaojian, “The Small Signal Stability Analysis of A Power System Integrated with PMSG-based Wind Farm”, IEEE Innovative Smart Grid Technologies – Asia (ISGT ASIA), Guangxi University, Nanning, China, 2014.
- [53] Muna Hameed Khalaf, Ch. Punya Sekhar, “Controlling of Solar Photovoltaic Inverters in Different Modes”, International Journal of Science and Research (IJSR), Nagarjuna University, Andhra Pradesh, India, 2013.

- [54] Ye Tang, Rolando Burgos, Chi Li and Dushan Boroyevich," Impact of PV Inverter Generation on Voltage Profile and Power Loss in Medium Voltage Distribution Systems", Center for Power Electronics Systems (CPES) — The Bradley Department of Electrical and Computer Engineering, IEEE, PP. 1869-1874, Virginia, USA, 2016.
- [55] Sirine Essallah, Adel Bouallegue and Adel Khedher," Optimal Placement of PV-Distributed Generation units in radial distribution system based on sensitivity approaches" 16th international conference on Sciences and Techniques of Automatic control & computer engineering - STA'2015, Monastir, Tunisia, December 21-23, 2015.
- [56] Devender Singh, R. K. Misra, and Deependra Singh, " Effect of Load Models In Distributed Generation Planning " IEEE Transactions on Power Systems, Vol.22, No. 4, November 2007



APPENDICES

1. Appendix-A : Lines and loads data of the 33-bus radial distribution network	72
2. Appendix-B : Power Flow Report of the network (without SSG).....	73
3. Appendix C : FC-SSG standard parameters	77
4. Appendix D : Eigenvalue Report of the a FC-SSG	82



Appendix-A: Lines and Loads Data of the 33-Bus Radial Distribution Network

Lines parameter and load data for 33 bus system (Singh *et al*, 2007).

Base Power = 1 MVA Base Voltage = 12.66 KV

Table A.1: Lines and loads data of the 33-bus radial distribution network.

From	To	LINE IMPEDANCE P.U		Line	S line p.u	Load on to bus p.u	
		R p.u	X p.u			P p.u	Q p.u
1	2	0.000575	0.000293	1	4.60	0.10	0.06
2	3	0.003076	0.001566	6	4.10	0.09	0.04
3	4	0.002279	0.001161	11	2.90	0.12	0.08
4	5	0.002373	0.001209	12	2.90	0.06	0.03
5	6	0.005100	0.004402	13	2.90	0.06	0.02
6	7	0.001166	0.003853	22	1.50	0.20	0.10
7	8	0.004430	0.001464	23	1.05	0.20	0.10
8	9	0.006413	0.004608	25	1.05	0.06	0.02
9	10	0.006501	0.004608	27	1.05	0.06	0.02
10	11	0.001224	0.000405	28	1.05	0.045	0.03
11	12	0.002331	0.000771	29	1.05	0.06	0.035
12	13	0.009141	0.007192	31	0.50	0.06	0.035
13	14	0.003372	0.004439	32	0.45	0.12	0.08
14	15	0.003680	0.003275	33	0.30	0.06	0.01
15	16	0.004647	0.003394	34	0.25	0.06	0.02
16	17	0.008026	0.010716	35	0.25	0.06	0.02
17	18	0.004538	0.003574	36	0.10	0.09	0.04
2	19	0.001021	0.000974	2	0.50	0.09	0.04
19	20	0.009366	0.008440	3	0.50	0.09	0.04
20	21	0.002550	0.002979	4	0.21	0.09	0.04
21	22	0.004414	0.005836	5	0.11	0.09	0.04
3	23	0.002809	0.001920	7	1.05	0.09	0.05
23	24	0.000559	0.004415	8	1.05	0.42	0.20
24	25	0.005579	0.004366	9	0.50	0.42	0.20
6	26	0.001264	0.000644	14	1.50	0.06	0.025
26	27	0.001770	0.000901	15	1.50	0.06	0.025
27	28	0.006594	0.005814	16	1.50	0.06	0.02
28	29	0.005007	0.004362	17	1.50	0.12	0.07
29	30	0.003160	0.001610	18	1.50	0.20	0.60
30	31	0.006067	0.005996	19	0.50	0.15	0.07
31	32	0.001933	0.002253	20	0.50	0.21	0.10
32	33	0.002123	0.003301	21	0.10	0.06	0.04

Appendix-B: Power Flow Report of the network (without SSG)

Table B.1: Power flow report of the network (without SSG).

P S A T 2.1.6

Author: Federico Milano, (c) 2002-2010
 e-mail: Federico.Milano@uclm.es
 website: <http://www.uclm.es/area/gsee/web/Federico>

File: C:\Users\Inspiron\Desktop\WEAM TAMIMI\PIDG3.mdl
 Date: 10-Apr-2017 18:38:43

NETWORK STATISTICS

Buses: 33
 Lines: 32
 Generators: 1
 Loads: 32

SOLUTION STATISTICS

Number of Iterations: 4
 Maximum P mismatch [p.u.] 0
 Maximum Q mismatch [p.u.] 0
 Power rate [MVA] 1

POWER FLOW RESULTS

Bus	V [p.u.]	phase [deg]	P gen [p.u.]	Q gen [p.u.]	P load [p.u.]	Q load [p.u.]
Bus1	0.99705	0.01364	0	0	0.1	0.06
Bus10	0.94986	0.11151	0	0	0.06	0.02
Bus11	0.94642	-0.11892	0	0	0.2	0.1
Bus12	0.9416	-0.08551	0	0	0.2	0.1
Bus13	0.93539	-0.16179	0	0	0.06	0.02
Bus14	0.92963	-0.22724	0	0	0.06	0.02
Bus15	0.92877	-0.22054	0	0	0.045	0.03
Bus16	0.92728	-0.20995	0	0	0.06	0.035
Bus17	0.92122	-0.30384	0	0	0.06	0.035
Bus18	0.91898	-0.38315	0	0	0.12	0.08
Bus19	0.91758	-0.42145	0	0	0.06	0.01
Bus2	1	0	3.9111	2.4053	0	0
Bus20	0.91622	-0.4453	0	0	0.06	0.02
Bus21	0.91421	-0.52301	0	0	0.06	0.02
Bus22	0.91361	-0.53276	0	0	0.09	0.04
Bus23	0.94794	0.15034	0	0	0.06	0.025
Bus24	0.94539	0.20573	0	0	0.06	0.025
Bus25	0.934	0.28646	0	0	0.06	0.02

Table B.1 (Continued): Power flow report of the network (without SSG).

Bus26	0.92583	0.36289	0	0	0.12	0.07
Bus27	0.92228	0.46722	0	0	0.2	0.6
Bus28	0.91814	0.38219	0	0	0.15	0.07
Bus29	0.91723	0.35905	0	0	0.21	0.1
Bus3	0.98301	0.09156	0	0	0.09	0.04
Bus30	0.91695	0.35128	0	0	0.06	0.04
Bus31	0.97945	0.06076	0	0	0.09	0.05
Bus32	0.97716	-0.14822	0	0	0.42	0.2
Bus33	0.97386	-0.19161	0	0	0.42	0.2
Bus4	0.97549	0.14756	0	0	0.12	0.08
Bus5	0.96813	0.21128	0	0	0.06	0.03
Bus6	0.99652	0.00264	0	0	0.09	0.04
Bus7	0.99297	-0.06554	0	0	0.09	0.04
Bus8	0.99227	-0.08508	0	0	0.09	0.04
Bus9	0.99164	-0.10551	0	0	0.09	0.04

LINE FLOWS

From Bus	To Bus	Line	P Flow [p.u.]	Q Flow [p.u.]	P Loss [p.u.]	Q Loss [p.u.]
Bus1	Bus2	1	-3.899	-2.4001	0.01212	0.00518
Bus3	Bus1	2	-3.3865	-2.1579	0.05132	0.02515
Bus13	Bus12	3	-0.68423	-0.30923	0.00413	0.00209
Bus15	Bus14	4	-0.56016	-0.26829	0.00055	-0.00068
Bus16	Bus15	5	-0.51429	-0.23886	0.00087	-0.00057
Bus17	Bus16	6	-0.45166	-0.20264	0.00264	0.00122
Bus19	Bus18	7	-0.27058	-0.08806	0.00035	-0.00053
Bus20	Bus19	8	-0.2103	-0.0787	0.00028	-0.00064
Bus21	Bus20	9	-0.15005	-0.05921	0.00025	-0.0005
Bus22	Bus21	10	-0.09	-0.04	5e-005	-0.00079
Bus24	Bus23	11	-0.88465	-0.94032	0.0033	0.00078
Bus25	Bus24	12	-0.81345	-0.90632	0.0112	0.009
Bus4	Bus3	13	-2.3419	-1.6541	0.01968	0.00948
Bus26	Bus25	14	-0.74567	-0.88042	0.00777	0.00591
Bus27	Bus26	15	-0.62181	-0.8093	0.00387	0.00112
Bus28	Bus27	16	-0.42022	-0.20858	0.00158	0.00072
Bus29	Bus28	17	-0.27001	-0.13918	0.00021	-0.0006
Bus10	Bus5	18	-2.1056	-1.5039	0.03784	0.03174
Bus14	Bus13	19	-0.62071	-0.2876	0.00352	0.00162
Bus23	Bus10	20	-0.94795	-0.9661	0.00258	0.00041
Bus18	Bus17	21	-0.39093	-0.16754	0.00072	0.0001
Bus3	Bus31	22	0.93492	0.45428	0.00314	0.00118
Bus31	Bus32	23	0.84178	0.4031	0.00051	0.00305
Bus5	Bus4	24	-2.2034	-1.5656	0.01849	0.00848
Bus32	Bus33	25	0.42127	0.20004	0.00127	4e-005
Bus30	Bus29	26	-0.06	-0.04	1e-005	-0.00082
Bus6	Bus1	27	-0.36097	-0.15796	0.00016	-0.00084
Bus7	Bus6	28	-0.27014	-0.1182	0.00082	-0.00025
Bus8	Bus7	29	-0.18004	-0.07907	0.0001	-0.00087
Bus9	Bus8	30	-0.09	-0.04	4e-005	-0.00093
Bus11	Bus10	31	-1.0932	-0.51201	0.0019	0.00537
Bus12	Bus11	32	-0.88836	-0.41132	0.00479	0.00069

GLOBAL SUMMARY REPORT

TOTAL GENERATION

REAL POWER [p.u.] 3.9111
 REACTIVE POWER [p.u.] 2.4053

TOTAL LOAD

REAL POWER [p.u.] 3.715
 REACTIVE POWER [p.u.] 2.3

TOTAL LOSSES

REAL POWER [p.u.] 0.19608
 REACTIVE POWER [p.u.] 0.10532

Table B.2: CPF Report.

P S A T 2.1.6

Author: Federico Milano, (c) 2002-2010
e-mail: Federico.Milano@uclm.es
website: <http://www.uclm.es/area/gsee/web/Federico>

File: C:\Users\Inspiron\Desktop\WEAM TAMIMI\PIDG3.mdl
Date: 10-Apr-2017 18:42:00

NETWORK STATISTICS

Buses:	33
Lines:	32
Generators:	1
Loads:	32

SOLUTION STATISTICS

Number of Iterations:	50
Maximum P mismatch [p.u.]	0
Maximum Q mismatch [p.u.]	0
Power rate [MVA]	1

GLOBAL SUMMARY REPORT

TOTAL GENERATION

REAL POWER [p.u.]	21.794
REACTIVE POWER [p.u.]	14.0535

TOTAL LOAD

REAL POWER [p.u.]	13.4698
REACTIVE POWER [p.u.]	8.3393

TOTAL LOSSES

REAL POWER [p.u.]	8.3242
REACTIVE POWER [p.u.]	5.7142

Table B.3: Loading parameter report (without SSG).

C Legend:						
C Loading	Parameter	λ (p.u.),	V_{Bus10} ,	V_{Bus2} ,	V_{Bus22} ,	V_{Bus30} ,
C Data:						
	0.00000	1.00019	1.00000	1.00044	1.00028	
	0.13665	0.99372	1.00000	0.98934	0.98962	
	0.27107	0.98725	1.00000	0.97821	0.97894	
	0.40326	0.98076	1.00000	0.96705	0.96822	
	0.53320	0.97427	1.00000	0.95586	0.95748	
	0.66088	0.96777	1.00000	0.94463	0.94671	
	0.78630	0.96126	1.00000	0.93337	0.93591	
	0.90944	0.95474	1.00000	0.92208	0.92507	
	1.03030	0.94821	1.00000	0.91075	0.91421	
	1.14885	0.94167	1.00000	0.89938	0.90330	
	1.26510	0.93512	1.00000	0.88797	0.89236	
	1.37901	0.92856	1.00000	0.87651	0.88138	
	1.49058	0.92198	1.00000	0.86502	0.87036	
	1.59979	0.91539	1.00000	0.85347	0.85930	
	1.70663	0.90879	1.00000	0.84188	0.84820	
	1.81106	0.90217	1.00000	0.83024	0.83705	
	1.91307	0.89554	1.00000	0.81854	0.82586	
	2.01264	0.88890	1.00000	0.80680	0.81461	
	2.10975	0.88223	1.00000	0.79499	0.80332	
	2.20436	0.87555	1.00000	0.78312	0.79197	
	2.29645	0.86886	1.00000	0.77119	0.78056	
	2.38599	0.86214	1.00000	0.75920	0.76910	
	2.47294	0.85540	1.00000	0.74713	0.75757	
	2.55727	0.84865	1.00000	0.73499	0.74598	
	2.63895	0.84187	1.00000	0.72278	0.73432	
	2.71793	0.83507	1.00000	0.71049	0.72260	
	2.79416	0.82824	1.00000	0.69811	0.71080	
	2.86761	0.82139	1.00000	0.68564	0.69892	
	2.93822	0.81452	1.00000	0.67308	0.68696	
	3.00592	0.80761	1.00000	0.66042	0.67492	
	3.07068	0.80068	1.00000	0.64766	0.66279	
	3.13240	0.79372	1.00000	0.63479	0.65057	
	3.19104	0.78673	1.00000	0.62181	0.63825	
	3.24650	0.77971	1.00000	0.60870	0.62584	
	3.29871	0.77265	1.00000	0.59547	0.61331	
	3.34757	0.76556	1.00000	0.58209	0.60068	
	3.39298	0.75844	1.00000	0.56858	0.58793	
	3.43484	0.75128	1.00000	0.55491	0.57506	
	3.47301	0.74408	1.00000	0.54108	0.56207	
	3.50738	0.73684	1.00000	0.52707	0.54896	
	3.53781	0.72957	1.00000	0.51289	0.53571	
	3.56413	0.72226	1.00000	0.49850	0.52233	
	3.58619	0.71492	1.00000	0.48391	0.50882	
	3.60381	0.70754	1.00000	0.46910	0.49517	

Appendix C: FC-SSG standard parameters

Table C.1: FC-SSG standard parameters.

Sofc (mask)	
This block defines a Solid Oxide Fuel Cell:	
Parameters	
DC Power and Voltage Rating [MW, kV]	[2 12.66]
Electrical and fuel processor response times (Te, Tf) [s, s]	[0.8 5]
Response times TH2, TH2O and TO2 [s, s, s]	[26.1 78.3 2.91]
Valve molar constants KH2, KH2O and KO2	[8.43e-4 2.81e-4 2.52e-3]
Constant Kr, ohmic loss [Ohm] and hydrogen to oxygen ratio rH_O	[0.996e-6 0.126 1.145]
Fuel optimization constants Uopt, Umax and Umin	[0.85 0.9 0.8]
Number of cells N0 and ideal standard potential E0 [V]	
[384 1.18]	
Gas absolute temperature T [K]	1273
Transformer reactance Xt [p.u.]	0.1
Gain and Time constant for Voltage Control Km, Tm [p.u. s]	[100 10]
Max and Min tap ratio [p.u./p.u. p.u./p.u.]	[1.2 0.8]
Control Mode: [0] constant current; [1] constant power	1
<input checked="" type="checkbox"/> Connected	

Table C.2: CSWTIG Model parameters.

Cswt (mask)

This block defines a constant speed wind turbine with third order asynchronous generator and dynamic shaft.

Parameters

Power, Voltage and Frequency Ratings [MVA, kV, Hz]
[2 0.690 50]

Stator Resistance Rs and Reactance Xs [p.u. p.u.]
[0.048 0.075]

Rotor Resistance Rr and Reactance Xr [p.u. p.u.]
[0.018 0.12]

Magnetization Reactance Xm [p.u.]
3.8

Inertia Constants Hwr Hm and Ks [kWs/kVA kWs/kVA p.u.]
[2.5 0.5 0.3]

Number of poles p and gear box ratio [int -]
[6 1/89]

Blade length and number [m int]
[75.00 3]

Number of machine that compose the park
1

Connected

Table C.3: Wind model parameters.

Wind (mask)
This block defines wind models for use with wind turbines.
Parameters
Number of output ports
<input type="text" value="1"/>
Wind model type <input type="text" value="weibull"/>
Nominal wind speed [m/s]
<input type="text" value="15"/>
Air density rho [kg/m ³]
<input type="text" value="1.225"/>
Filter time constant tau [s]
<input type="text" value="10"/>
Sample time for wind measures [s]
<input type="text" value="0.1"/>
Weibull distribution constants C and K
<input type="text" value="[20 2]"/>
Wind ramp constants Tsr, Ter and Awr [s s m/s]
<input type="text" value="[5 15 1]"/>
Wind gust constants Tsg, Teg and Awg [s s m/s]
<input type="text" value="[5 15 1]"/>
Wind turbulence constants h, z0, df and n [m - Hz int]
<input type="text" value="[50 0.01 0.2 50]"/>
Mexican hat wavelet time center and shape factor
<input type="text" value="[10 1]"/>

Table C.4: Synchronous generator model parameters.

Syn (mask)
This block defines a fourth order synchronous machine.

Parameters

Power, voltage and frequency ratings [MVA, kV, Hz]
[2 12.66 50]

Machine Dynamic Order

resistance r_a and leakage reactance x_l [p.u. p.u.]
[0.001 0.05]

d-axis reactances X_d , X'_d , X''_d [p.u.,p.u.,p.u.]
[1.90 0.302 0.204]

d-axis open circuit time constants T'_{d0} and T''_{d0} [s, s]
[8.00 0.04]

q-axis reactances X_q , X'_q , X''_q [p.u. p.u. p.u.]
[1.70 0.50 0.30]

q-axis open circuit time constants T'_{q0} and T''_{q0} [s s]
[0.80 0.02]

Inertia ($M = 2H$) and Damping [s, p.u.]
[10.00 0.00]

Speed and active power additional signals K_w and K_p [p.u., p.u.]
[0.00 0.00]

Percentage of active and reactive powers at bus [p.u. p.u.]
[1.00 1.00]

d-axis additional circuit leakage time constant T_{aa} [s]
0.002

Saturation coefficients $S(1.0)$ and $S(1.2)$
[0 0]

Number of input signals

COI number
1

Connected

Table C.5: AVR model settings.

Exc (mask)
This block defines an Automatic Voltage Regulator.

Parameters

Automatic Voltage Regulator Type

Maximum Regulator Voltage [p.u.]

Minimum Regulator Voltage [p.u.]

Regulator Gain m0 [p.u./p.u.]

First Regulator Pole T1 [s]

First Regulator Zero T2 [s]

Second Regulator Pole T3 [s]

Second Regulator Zero T4 [s]

Time Constant of the Field Circuit Td [s]

Time Delay of the Measurement System Tr [s]

Coefficient of the Ceiling Function (A B)

Number of input signals

Connected

Appendix-D: Eigenvalue Report of the a FC-SSG

Table D.1: Eigenvalue report of the a FC-SSG.

```

EIGENVALUE REPORT
P S A T 2.1.6
Author: Federico Milano, (c) 2002-2010
e-mail: Federico.Milano@uclm.es
website: http://www.uclm.es/area/gsee/web/Federico
File: C:\Users\Inspiron\Desktop\WEAM TAMIMI\System with FC-Generator\PIDGFuel.mdl
Date: 24-May-2017 12:47:08

STATE MATRIX EIGENVALUES
Eigenvalue      Most Associated States      Real part      Imag. Part      Pseudo-Freq.      Frequency
Eig As #1      m_Sofc_1                    -1.5566        0                0                0
Eig As #2      vk_Sofc_1                    -1000.0001     0                0                0
Eig As #3      Ik_Sofc_1                    -1.2906        0                0                0
Eig As #4      pO2_Sofc_1                   -0.26958       0                0                0
Eig As #5      qH2_Sofc_1                   -0.22641       0                0                0
Eig As #6      pH2_Sofc_1                   -0.04604       0                0                0
Eig As #7      pH2O_Sofc_1                  -0.012         0                0                0

PARTICIPATION FACTORS (Euclidean norm)
                Ik_Sofc_1      vk_Sofc_1      pH2_Sofc_1      pH2O_Sofc_1      pO2_Sofc_1
Eig As #1      0              0              0              0              0
Eig As #2      0              1              0              0              0
Eig As #3      0.95573       4e-005        0.01432        0.00067        0.02127
Eig As #4      0.02996       3e-005        0.04738        0.00052        0.54634
Eig As #5      0.01612       2e-005        0.08714        0.0004         0.28125
Eig As #6      0.00508       1e-005        0.86673        0.00521        0.00139
Eig As #7      0.00052       0              0.00364        0.99297        8e-005

PARTICIPATION FACTORS (Euclidean norm)
                qH2_Sofc_1      m_Sofc_1
Eig As #1      0              1
Eig As #2      0              0
Eig As #3      0.00797       0
Eig As #4      0.37577       0
Eig As #5      0.61508       0
Eig As #6      0.12159       0
Eig As #7      0.0028        0

STATISTICS
DYNAMIC ORDER                7
# OF EIGS WITH Re(mu) < 0    7
# OF EIGS WITH Re(mu) > 0    0
# OF REAL EIGS                7
# OF COMPLEX PAIRS            0
# OF ZERO EIGS                0

```


Table D.2: Eigenvalue report of the Synch.SSG.

```

EIGENVALUE REPORT
P S A T 2.1.6
Author: Federico Milano, (c) 2002-2010
e-mail: Federico.Milano@uclm.es
website: http://www.uclm.es/area/gsee/web/Federico

File: C:\Users\Inspiron\Desktop\WEAM TAMIMI\System with Sync-Generator\SyncDG.mdl
Date: 24-May-2017 14:17:41

STATE MATRIX EIGENVALUES
Eigenvalue      Most Associated States      Real part      Imag. Part      Pseudo-Freq.      Frequency
Eig As # 1      vr2_Exc_1                  -1             0               0                 0
Eig As # 2      vr1_Exc_1                  -10            0               0                 0
Eig As # 3      vm_Exc_1                   -1000          0               0                 0
Eig As # 4      psid_Syn_1, psiq_Syn_1    -37.2678       334.4118        53.2232           53.5527
Eig As # 5      psid_Syn_1, psiq_Syn_1    -37.2678       -334.4118       53.2232           53.5527
Eig As # 6      e2d_Syn_1                  -81.4277       0               0                 0
Eig As # 7      e2q_Syn_1                  -35.9937       0               0                 0
Eig As # 8      delta_Syn_1, omega_Syn_1  -0.88771      10.3151         1.6417            1.6478
Eig As # 9      delta_Syn_1, omega_Syn_1  -0.88771      -10.3151        1.6417            1.6478
Eig As #10     e1d_Syn_1                  -2.9506        0               0                 0
Eig As #11     e1q_Syn_1                  -0.66004       0               0                 0
Eig As #12     vf_Exc_1                   -1.1455        0               0                 0

PARTICIPATION FACTORS (Euclidean norm)
Eigenvalue      delta_Syn_1      omega_Syn_1      e1q_Syn_1      e1d_Syn_1      e2q_Syn_1
Eig As # 1      0                0                0                0                0
Eig As # 2      0                0                0                0                0
Eig As # 3      0                0                0                0                0
Eig As # 4      0.00043          8e-005           2e-005           0.00011         0.00284
Eig As # 5      0.00043          8e-005           2e-005           0.00011         0.00284
Eig As # 6      0.00401          0.00448          4e-005           0.03424         0.00231
Eig As # 7      0.00401          0.00273          0.01688          0.00017         0.97111
Eig As # 8      0.45512          0.45472          0.00237          0.05499          0.00503
Eig As # 9      0.45512          0.45472          0.00237          0.05499          0.00503
Eig As #10     0.0245           0.02617          0.01216          0.91008          0.00073
Eig As #11     0.00165          0.00081          0.96599          0.01534          0.01533
Eig As #12     0                0                0                0                0

PARTICIPATION FACTORS (Euclidean norm)
Eigenvalue      e2d_Syn_1      psiq_Syn_1      psid_Syn_1      vm_Exc_1      vr1_Exc_1
Eig As # 1      0                0                0                0                0
Eig As # 2      0                0                0                0                1
Eig As # 3      0                0                0                1                0
Eig As # 4      0.00545         0.49448         0.49659          0                0
Eig As # 5      0.00545         0.49448         0.49659          0                0
Eig As # 6      0.94589         0.00045         0.0086           0                0
Eig As # 7      0.00176         0.00311         0.00022          0                0
Eig As # 8      0.02094         0.0053          0.00153          0                0
Eig As # 9      0.02094         0.0053          0.00153          0                0
Eig As #10     0.02464         0.00105         0.00067          0                0
Eig As #11     0.0002          0.00068         2e-005           0                0
Eig As #12     0                0                0                0                0

PARTICIPATION FACTORS (Euclidean norm)
Eigenvalue      vr2_Exc_1      vf_Exc_1
Eig As # 1      1                0
Eig As # 2      0                0
Eig As # 3      0                0
Eig As # 4      0                0
Eig As # 5      0                0
Eig As # 6      0                0
Eig As # 7      0                0
Eig As # 8      0                0
Eig As # 9      0                0
Eig As #10     0                0
Eig As #11     0                0
Eig As #12     0                1

STATISTICS
DYNAMIC ORDER      12
# OF EIGS WITH Re(mu) < 0      12
# OF EIGS WITH Re(mu) > 0      0
# OF REAL EIGS      8
# OF COMPLEX PAIRS      2
# OF ZERO EIGS      0
    
```

Table D.3: Eigenvalue report of the CSWTIG.

EIGENVALUE REPORT - CSWTIG

P S A T 2.1.6

Author: Federico Milano, (c) 2002-2010
 e-mail: Federico.Milano@uclm.es
 website: http://www.uclm.es/area/gsee/Web/Federico

File: C:\Users\Inspiron\Desktop\WEAM TAMIMI\System with WTC SIG -DG\PIDwind.mdl
 Date: 24-May-2017 16:00:09

STATE MATRIX EIGENVALUES

Eigenvalue	Most Associated States	Real part	Imag. Part	Pseudo-Freq.	Frequency
Eig As #1	omega_m_Cswt_1, e1r_Cswt_1	0.20838	73.4935	11.6968	11.6969
Eig As #2	omega_m_Cswt_1, e1r_Cswt_1	0.20838	-73.4935	11.6968	11.6969
Eig As #3	e1m_Cswt_1	-0.98538	0	0	0
Eig As #4	omega_t_Cswt_1, gamma_Cswt	-0.26201	4.2964	0.68379	0.68506
Eig As #5	omega_t_Cswt_1, gamma_Cswt	-0.26201	-4.2964	0.68379	0.68506
Eig As #6	vw_Wind_1	-0.1	0	0	0

PARTICIPATION FACTORS (Euclidean norm)

	vw_Wind_1	omega_t_Cswt_1	omega_m_Cswt_1	gamma_Cswt_1	e1r_Cswt_1
Eig As #1	0	3e-005	0.49956	0.00878	0.47629
Eig As #2	0	3e-005	0.49956	0.00878	0.47629
Eig As #3	0	0.00061	0.00013	1e-005	0.02999
Eig As #4	0	0.49926	3e-005	0.49083	0.00841
Eig As #5	0	0.49926	3e-005	0.49083	0.00841
Eig As #6	1	0	0	0	0

PARTICIPATION FACTORS (Euclidean norm)

	e1m_Cswt_1
Eig As #1	0.01535
Eig As #2	0.01535
Eig As #3	0.96926
Eig As #4	0.00147
Eig As #5	0.00147
Eig As #6	0

STATISTICS

DYNAMIC ORDER	6
# OF EIGS WITH $\text{Re}(\mu) < 0$	4
# OF EIGS WITH $\text{Re}(\mu) > 0$	2
# OF REAL EIGS	2
# OF COMPLEX PAIRS	2
# OF ZERO EIGS	0

CURRICULUM VITAE

PERSONAL INFORMATION

Name, Surname : Weam Al- Tameemi
Nationality : Iraqi
Date and Place of Birth : 5 December 1978, Kirkuk-Iraq
Marital Status : Married
Phone : +90 5378738144
Email : soler.tamimi@yahoo.com



EDUCATION

High School : AL-Waleed Secondary School, 1996.
Undergraduate : College of Electrical Engineering / University of Mosul,
2001.

WORK EXPERIENCE

Year : 2003- Present
Place : Iraqi Ministry of Electricity/Electrical Power Production
Sector.

FOREIGN LANGUAGES

English, Turkish